Synthesis and Reactivity of Aluminum (III) Complexes Supported by Non-Innocent Bis(enol)amine and Di(imino)pyridine Ligands

By

NATHAN ANH PHAN

DISSERTATION

Submitted in partial satisfaction of the requirements for the degree of

Doctor of Philosophy

in

Chemistry

in the

OFFICE OF GRADUATE STUDIES

of the

UNIVERSITY OF CALIFORNIA

DAVIS

Approved:

Louise A. Berben, Chair

Alan L. Balch

Philip P. Power

Committee in Charge

2023

Nathan Anh Phan
July 2023
Chemistry

Synthesis and Reactivity of Aluminum (III) Complexes Supported by Non-Innocent Bis(enol)amine and Di(imino)pyridine Ligands

Abstract

This dissertation discusses the synthesis and characterization of aluminum(III) (Al^{3+}) complexes with the non-innocent ligands bis(enol)amine (H_3ONO) and di(imino)pyridine (I_2P). This work contributes to the rich history of main group coordination chemistry by exploring the capacity of these non-innocent ligand Al^{3+} complexes to activate small molecules through novel ligand-based proton-, electron-, and hydride-transfer reactions.

In chapter 2, a series of Al^{3+} complexes supported by the tridentate bis(enol)amine ligand (H_3ONO, 1,1'-azanediylbis(3,3-dimethylbutan-2-one) is coordinated to Al are synthesized and characterized. Reaction of $AlCl_3$ with singly deprotonated H_2ONO^- affords the pseudo-octahedral complex $[(H_2ONO^-)_2Al][AlCl_4]$ (**2.1**). Reaction of $AlCl_3$ with the doubly protonated $HONO^{2-}$ affords the five-coordinate, pseudo-trigonal bipyramidal complex $(HONO^{2-})AlCl(THF)$ (**2.2**). Reversible ligand-based protonation/deprotonation of the Al complexes is demonstrated by the deprotonation of **2.1** with Et_3N to afford **2.2** and the protonation of **2.2** with HCl to afford **2.1**. An attempt to deprotonate **2.2** with ^tBuOK yielded $[(HONO^{2-})Al](\mu\text{-}^tBuO)$ (**2.3**), with no change to the ligand protonation state. An intermolecular C—H bond activation reaction takes place when **2.2** reacts with two equivalents of TEMPO to afford $[(HONO^{2-})Al(TEMPO)(TEMPOH)]$ (**2.4**).

In Chapter 3, di(imino)pyridine (I_2P) Al^{3+} complexes are synthesized and characterized with ancillary unsupported primary phosphido ligands. (I_2P^{2-})AlI reacts with LiP(H)Mes to form (I_2P^{2-})Al(PHMes) (**3.1**) and (I_2P^{2-})AlI reacts with LiP(H)Ph to form (I_2P^{2-})Al(PHPh) (**3.2**). Solid-state structures reveal distorted tetrahedral geometry in **3.1** and **3.2** and single bond character in the Al—P bond. Near infrared spectra display low energy absorption bands near 1050 nm that are consistent with pincer ligand – Al charge transfer transitions and metalloaromatic character in the "(I_2P^{2-})Al" fragment of the molecules. The phosphido ligands lie out of the I_2P ligand plane by up to 15°, consistent with previous reports where π-donor halide ligands occupy a fourth coordination site on Al.

In Chapter 4, an electrochemical characterization of $V\{N(SiMe_3)_2\}_3$ (**4.**1) is presented. During the preparation of **4.1** a discrepancy between the observed violet color and the previously reported brown color prompted further investigation of the compound. As a result, electrochemical measurements are presented to contribute to the characterization of the purple compound.

Table of Contents

Acknowledgements

I would like to thank Professor Louise Berben for welcoming me into her research group and providing the opportunity to learn and grow as an independent research scientist. The 2015 version of myself that applied to grad school would be blown away to learn about the organometallic research I was able to accomplish. Under Louise's mentorship I worked on incredible projects in a great lab; I am thankful for my experience and I look forward to carrying on with all the lessons I have learned from my time in Davis.

I owe a lot to every iteration of labmates I've had over the years. Toby immediately welcomed me into the lab, teaching me how to think critically about my chemistry and outside the lab invited me to hang out with the senior grad students. Amela and Talia were incredible labmates, we had long discussions ranging from chemistry to the tv shows we were watching. Traveling with Thomas to San Diego for ACS was a grad school highlight, I'm glad he was able to tolerate me for a week, especially during the long drives. It was great to be around Leo and Amanda and their contagious "youthful" energy. I spent a lot of time with Santanu both around the lab and the restaurants downtown; it was wonderful to see him settle into the States. Working with Keyan kept the lab fresh and exciting, seeing his journey from gen chem student to now chemistry grad student has been remarkable.

There are many throughout the UCD chemistry department I have to thank that I'll try to fit into a paragraph. My friends and cohort members Alice, Chris, and Lucy were a fantastic support system as we all started at the same time and figured out every stage of grad school together. Whenever I had to TA I always put in a preference to work with Dr. Julia Chamberlain, a true role model whose unwavering positive attitude is something I try my best to match. Learning from Dr. Philip Power and Dr. Alan Balch during every big stage (QE, 3rd Year

Seminar, this dissertation) was an extremely valuable process. I am appreciative of collaborating with Dr. Clifton Wagner and running experiments with his beautifully colored compounds. It was a privilege to learn crystallography from Dr. Jim Fettinger, who was always accessible and helpful, and Dr. Marilyn Olmstead, who was kind enough to invite me, a confused 2nd year student, into her home to help solve a twinned crystal structure.

I would also like to thank all my chemistry professors at the University of Portland, as they helped me hit the ground running when I got to Davis. My undergraduate research with Dr. Eugene Urnezius completely shaped my future direction, from Dr. U I learned I wanted to pursue organometallic chemistry. I feel very lucky to have worked in his lab and have learned disciplined air-free Schlenk technique.

When I chose Davis, living 1.75 hours away from my hometown San Jose wasn't intentional but now looking back I can't imagine the last couple of years without it. I was very fortunate to be able to see my family so close by. I'm lucky enough to have parents who insisted I take homecooked meals back to Davis whenever I saw them. Every time I had to move or switch apartments, they offered to help me, their adult son. Thank you mom, dad, Nathalie, Mandy, and Janelle for being so supportive. I'm also grateful for my nephews and nieces Dom, Mav, and Kai who are all a joy to see grow up.

The last but most important person I want to thank is Bao Tran. Throughout the years you have been a constant source of compassion, support, and inspiration. It's also even true that without you I may not have passed some of my undergraduate chemistry courses… but the first part is more important! As of writing this we have already begun our "postgrad" future and I cannot wait to discover what's coming next with you together.

Glossary of Abbreviations

Abbreviations

am = amido

Ar = aryl

Ad = adamantyl

Bn = benzyl

CAACs = cyclic alkyl amino carbenes

C_6D_6 = deuterated benzene

C_6H_6 = benzene

Cp = cyclopentadiene

CV = cyclic voltammagramm

Diip = diisopropylphenyl

DMAP = *N*,*N*-dimethylaminopyridine

$DMAPH^+$ = *N*,*N*-dimethylaminopyridinium tetrafluoroborate

Et_3N = triethylamine

Et_3NH^+ = triethylammonium tetrafluoroborate

Et_2O = diethyl ether

EtOH = ethanol

Fc = ferrocene

Fc^+ = ferrocenium

GC = glassy carbon

GC-MS = gas chromatography mass spectrometry im = imine

^{i}Pr = isopropyl

K_2P = dibenzoylpyridine

MeOH = methanol

Mes = mesityl

MeCN = acetonitrile

NMR = nuclear magnetic resonance

Ph = phenyl

py = pyridyl

SCE = saturated calomel electrode

^{t}Bu = *t*-butyl

TEMPO = (2,2,6,6-Tetramethylpiperidin-1-yl)oxyl

THF = tetrahydrofuran

Chapter 1: Introduction

1.1 Motivation and Background. The fundamental and societal need for scientific investigation in exploratory chemical research is vast. The work presented in this dissertation will focus on the development of sustainable catalysis via exploratory organometallic synthesis. Achieving accessible and efficient sustainable catalysis is vital research needed to address the alarming rapid change in global climate and the allocation of Earth's natural resources.[1] To address these concerns, one area of research is expanding the function of non-precious metals into a nontraditional role of small molecule activation and catalysis. Utilizing aluminum as an organometallic platform for sustainable catalysis is attractive due to aluminum's abundance and unique chemical properties.

Aluminum (Al) is the most abundant metal in Earth's crust and is relatively non-toxic. Al is commonly known as a sturdy yet lightweight metal and has common industrial and everyday applications. In chemistry, Al is known to participate in a range of reactivity that is attributed to its Lewis acidic properties. As a lighter main group *p*-block metal, Al typically exists in the +3 oxidation state and consequently holds a high charge density. As a Lewis acid catalyst, Al has been well-established to perform organic transformations such as Friedel-Crafts reactions, Oppenauer oxidations, and reliably reducing common functional groups via Al hydrides. There has also been widespread work in using Al as an α-olefin polymerization catalyst.[2] Furthering the known reactivity of Al for sustainable catalysis is a desirable next step.

A key phase in developing catalytic systems is performing small molecule activation, which usually requires a redox transformation. There has been much progress on the development of redox chemistry with main group metals but not to the same extent as transition metals.[3,4] Transition metals can inherently perform redox chemistry due to their accessible metal-centered redox couple. Al under mild conditions does not have a metal-centered redox couple that is readily accessible. Recently there has been much progress in low-valent Al(I) complexes that can activate small molecules but their syntheses remain challenging and have limited stability.[5,6] In addition to low-valent Al complexes, other strategies to activate small molecules with main group elements include using Frustrated Lewis Pairs (FLPs)[7] and noninnocent ligands.

The work presented will focus on recent development of Al complexes with noninnocent ligands. It is a known strategy to use noninnocent ligands with the purpose of uncovering new reactions pathways for small molecule activation. These pathways include ligand-based proton-, electron-, and hydride-transfer, which can provide novel reactivity for Al complexes. The development of these new complexes as a fundamental study has elucidated new structures, bonding, and reactivity. The results have contributed to the rich history of Al chemistry and have provided insight into molecular organometallic design principle with main group metal Al and is working toward the goal of sustainable catalysis.

1.2 Organometallic Chemistry of Aluminum. The first organometallic Al complexes were discovered mid-19th century.[8] The early organometallic Al complexes featured σ-bonded aliphatic and halide groups surrounding a 3-4 coordinate metal center. These simple alkyl Al complexes are described by the AlR_3 formula where R can vary among aliphatic groups such as methyl, benzyl, *tert*-butyl, etc (Scheme 1.1). The bonding and geometry of these complexes vary on the size of the R substituent and their electronic contribution. For example, the less bulky trimethylaluminum and triethylalumium exist as dimers and feature bridging alkyl ligands.

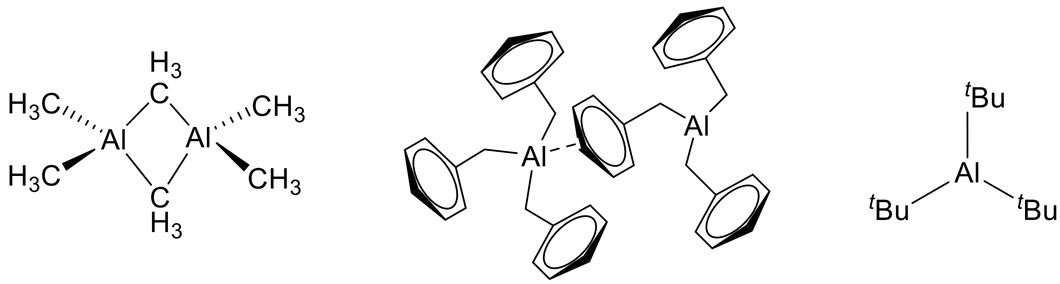

R = Me R = Bn R = ^{t}Bu

Scheme 1.1. Simple organoaluminum complexes with AlR_3 formula.

Alkyl Al compounds have a wide range of uses as chemical reagents. They are typically clear colorless liquids that are water-reactive and pyrophoric. Alkyl Al reagents are strongly reducing and can utilize their basic alkyl ligands to deprotonate acids and to alkylate substrates. Alkyl Al reagents have also demonstrated high performance in polymer catalysis.[9] Ziegler and Natta were awarded the Nobel Prize in Chemistry in 1963 for their contributions to the field, where the Al catalysts polymerized olefins.

The earliest multidentate chelating ligand complexes of Al were developed in the 1960's. S. Herzhog reported the first synthesis of Al complex with bidentate ligand bipyridine in 1963.[10] Joyce Corey further developed bipyridine Al halide complexes, along with phenanthroline and terpyridine ligands, in 1977 (Scheme 1.2).[11] Other noteworthy early multidentate ligand Al complexes include the incorporation of catechol-[12], diethylenetriamine-[13], aminophenol-based[14] ligands. These early complexes were initially notable for their structural properties in comparison to prior transition metal analogues. Their syntheses were instrumental for influencing future Al complexes that have applications toward activating small molecules were later developed.

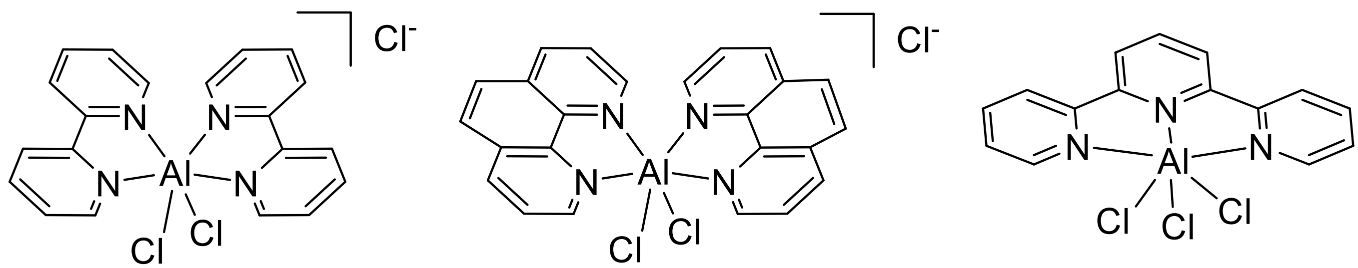

Scheme 1.2. Early multidentate chelating ligand complexes of Al featuring bipyridine (left), phenanthroline (center), and terpyridine (right) ligands.

A few examples of the reactivity of early multidentate ligand Al complexes demonstrated include CO_2 activation, mixed-alkyl ligand exchange, and ring opening polymerization. Inoue reported the activation of CO_2 with Al porphyrin complexes (Scheme 1.3).[15] With ancillary alkoxide ligands, Inoue's complexes activated CO_2 via insertion into the Al—O bond. Darensbourg reported the synthesis of novel tris-pyrazolyl hydroborate Al complexes that catalyzed the coupling of CO_2 with epoxides to form cyclic carbonates (Scheme 1.3).[16] Smith reported the initial synthesis of a β-diketiminato Al complex that demonstrated unusual exchange of alkyl ligands (Scheme 1.3).[17] β-diketiminato Al complexes later became a common motif to support low-valent Al, which has since exhibited a further range of reactivity.[5]

Another noteworthy example of a multidentate ligand Al complex with interesting reactivity is Bertrand's Al complex flanked by a diamidoamine ligand (Scheme 1.3).[18] Bertrand's trigonal-monpyramidal Al complex catalyzed the ring-opening polymerization of propylene oxide and (D,L)-Lactide. The reactivity of the complex is attributed to the complex's unusual geometry and the empty axial coordination site which is utilized for substrate binding at the Lewis acidic Al center. Bertrand's complex was also capable of being protonated by the addition of one equivalent of HCl at the amido position of the diamidoamine ligand. The ligand's basicity foreshadows future work with Al and non-innocent ligands where ligand-based proton-transfer is explored.

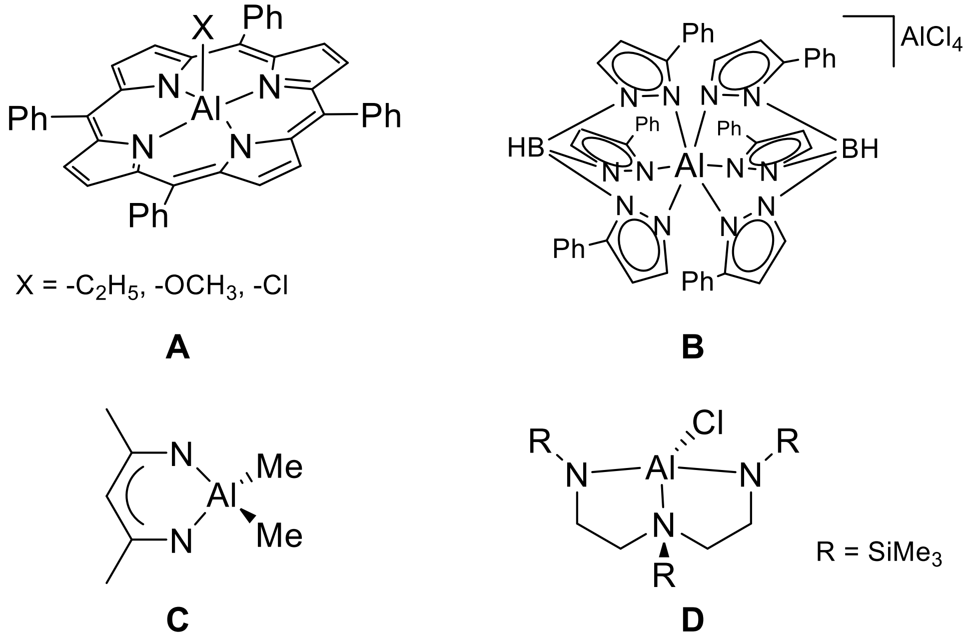

Scheme 1.3. Select examples of multidentate ligand Al complexes with a diverse range of reactivity, featuring porphyrin (**A**), tris-pyrazolyl hydroborate (**B**), β-diketiminato (**C**), and diamidoamine (**D**) ligands.

In the 2010's, Al-based Frustrated Lewis Pairs (FLP) became increasingly common in organometallic Al chemistry. FLPs are a class of compounds that contain sterically separated Lewis acidic and Lewis basic components. Due to having two reactive sites, FLPs have shown an impressive range of the dipolar activation of small molecules.[19] The majority of FLP chemistry has been based on using boron Lewis acids but has been recently expanded to Al and other Lewis acids. Chen has reported the rapid polymerization of methyl methacrylate, pairing

Lewis Acid $Al(C_6F_5)_3$ with either N-heterocyclic carbenes or phosphine Lewis bases.[20] Uhl has reported the activation of terminal acetylenes and reversible binding of CO_2 with Al—P based FLPs.[21]

More recently low-valent Al coordination complexes have also become a class of Al-based compounds that can exhibit a range of reactivity toward small molecules.[22] Unlike FLPs, low-valent Al compounds' reactivity are attributed to redox processes with the Al(I)/Al(III) redox couple. The first stable low-valent Al compound reported was in 1991 by Schnöckel, a tetrameric Al cluster.[23] The second reported low-valent Al compound reported was an organometallic β-diketiminato two-coordinate complex synthesized by Roesky.[24] The β-diketiminato Al(I) complex has since been discovered to have a rich set of reactivity, being able to activate CO, CO_2, alkenes, and cleave C—H bonds.[25]

Al(I) chemistry has since been expanded when Aldridge reported the synthesis of the first nucleophilic aluminyl anion in 2018.[26] Al(III) compounds are known for their reactivity as Lewis acids and electrophiles. The discovery of nucleophilic aluminyl anions provided an expansion of what is traditionally expected from Al coordination complexes with respect to both synthesis and reactivity. The formally Al(I) complex is supported by a tridentate diamido-dimethylxanthene ligand (Scheme 1.4). Aldridge's compound has demonstrated remarkable reactivity, even reversibly activating the C—C bonds of benzene at room temperature.[27] Soon after Aldridge's initial work, additional nucleophilic aluminyl anions were synthesized with differing ligand scaffolds. Diamido *N,N'*-heterocyclic nucleophilic aluminyl anions were reported by Coles[28] and Hill (Scheme 1.4).[29] Alkyl substituted ligands were reported by Yamashita[30] and Kinjo[31], bearing cyclic (alkyl)(amino) ligands substituted by an aluminyl.

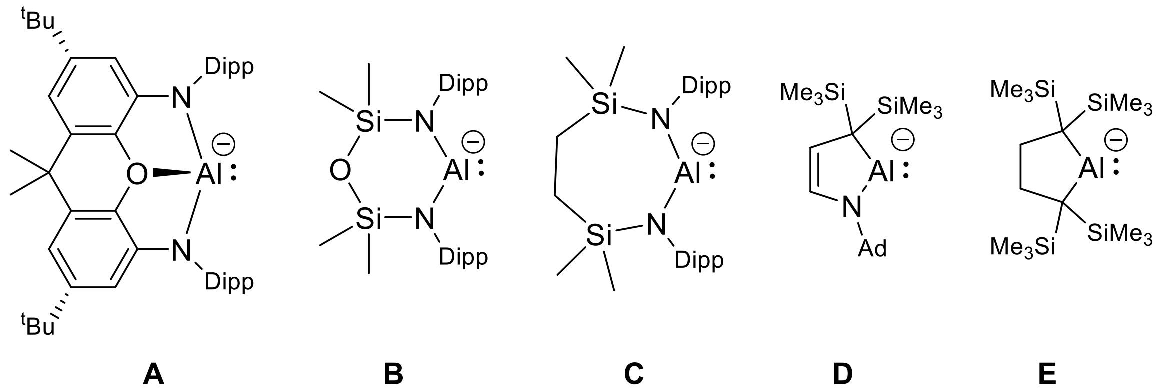

Scheme 1.4. Nucleophilic aluminyl anions reported by Aldridge (A), Coles (B), Hill (C), Yamashita (D), and Kinjo (E).

1.3 Non-Innocent Ligands. Non-innocent ligands are ligands that have ambiguous charge states because they can coordinate to metals in multiple possible charge states. This is contrary to “innocent" ligands where charge states are obvious due to only a single charge state being accessible. Determining the charge state of a non-innocent ligand can further be complicated when the metal center of the coordination complex also has several accessible oxidation states. Crystallographic and spectroscopic measurements are used to determine and confirm the charge states of non-innocent ligand. An example of a non-innocent ligand is the catechol-quinone moiety (Scheme 1.5). When complexed to a metal, the ligand scaffold can support various protonation and charge states.

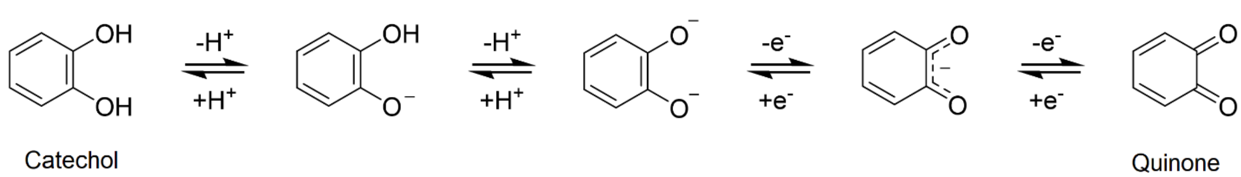

Scheme 1.5. Redox and protonation series of the non-innocent catechol-quinone moiety.

The first transition metal complexes with non-innocent ligands initially attracted interest for being a unique class of chemical compounds. Nickel dithiolene complexes reported by Schrauzer and Mayweg featured an electronic structure that was accepted to be Ni^{2+} in square planar geometry with each dithiolene ligand singly reduced with a radical.[32] Soon afterward other dithiolene transition metal complexes were synthesized and other non-innocent ligands such as quinones and amido phenolates.[33]

The utility of non-innocent ligand transition metal complexes expanded when redox transfer reactions were developed with the platform. Redox transformations facilitated by non-innocent-ligand complexes allow for more advanced reaction mechanisms than using a metal alone.[34] Non-innocent ligands facilitate ligand-based electron-transfer whereas the redox processes of traditional transition metal complexes are metal centered. Scheme 1.6 depicts a remarkable example of a non-innocent ligand iron complex that “cycles” between ligand charge states when transferring electrons.[35,36] The formally Fe^{II} complex catalyzes the [2 + 2] cycloaddition reaction, where electron-transfer takes place between ligand and substrate. The fluctuating charge state of the ligand also modifies the Lewis acidity of the Fe complex, allowing the substrate’s ring-closing reaction to occur at the metal center.

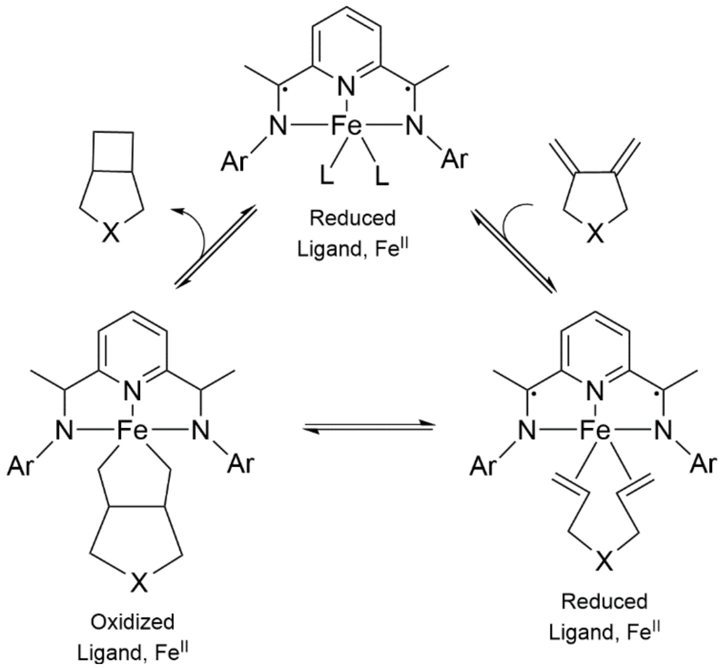

Scheme 1.6 A non-innocent 2,6-diiminepyridine ligand iron complex catalyzes [2 + 2] cycloaddition ring-closure reactions through a ligand-substrate electron-transfer pathway.

Non-innocent ligands have also been recognized in bioinorganic chemistry. Metalloenzymes have been known to facilitate redox reactions such as the reduction of dioxygen to superoxide and peroxides.[37] Initially these catalytic reactions and their products were known but their reaction mechanisms were poorly understood. With advances in spectroscopy, theoretical methods, and model chemistry to develop synthetic models, the nuances in the reaction mechanism of $Cu\text{-}O_2$ complexes were elucidated.[38] Another example of non-innocent ligand in a metalloenzyme is galactose oxidase.[39] Galactose oxidase, a copper-centered protein, catalyzes the oxidation of *D*-galactose, utilizing a non-innocent tyrosine ligand to facilitate electron transfer (Scheme 1.7).[40] Galactose oxidase has inspired model complexes with similar non-innocent ligand scaffolds and those have shown catalytic reactivity as well (Scheme 1.7).[41]

Non-innocent ligands in bionorganic chemistry serve as an inspiration for ligand design as well as showcasing possible reactivity in discovering new reaction mechanisms.

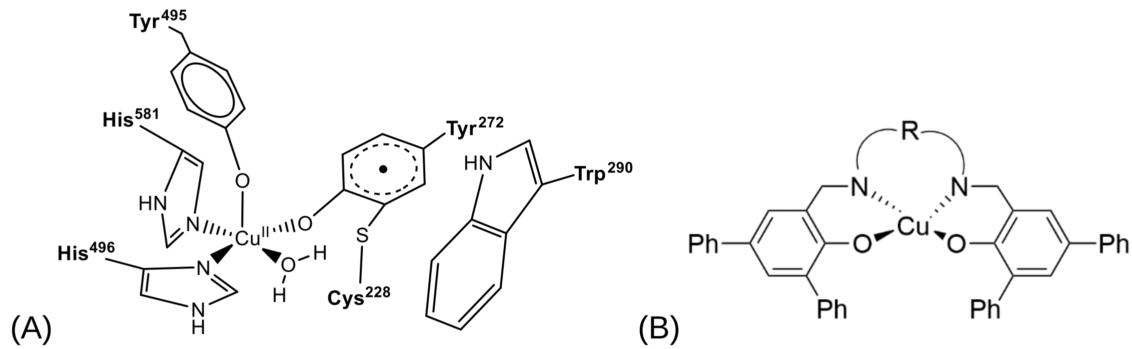

Scheme 1.7 (A) Copper center of metalloenzyme galactose oxidase. The tyrosine ligand serves as a noninnocent ligand, shuttling electrons. (B) Copper complex model compound with a tetradentate non-innocent ligand. The complex can reduce primary alcohols to aldehydes.

An example of bioinorganic chemistry influencing ligand design in main group coordination chemistry is a dihydropyridnate Al complex (Scheme 1.8, right).[42] In biological systems, NADH (nicotinamide adenine dinucleotide), an organic cofactor, participate in proton-, electron, and hydride-transfer reactions with regioselectivity (Scheme 1.8, left). The dihydropyridinate Al complex was synthesized to explore potential ligand-based hydride-transfer, a reaction pathway that could expand upon accessible hydride-transfer selectivity.

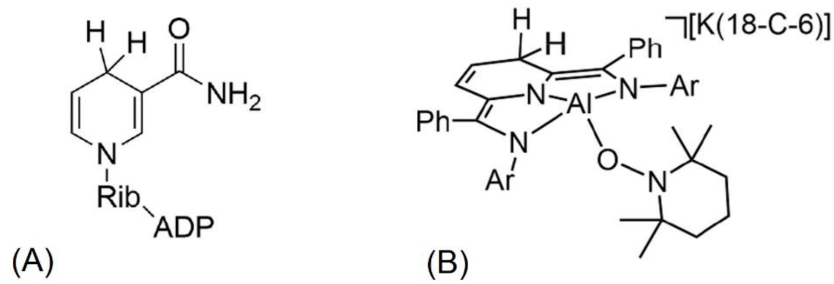

Scheme 1.8 (A) Organic cofactor NADH (nicotinamide adenine dinucleotide) (B) Dihydropyridnate Al complex

1.5 Outlook.

The aim of the work presented is to develop Al complexes from the elementary steps of molecular design to ultimately discover new chemical reactivity in catalytic systems. The combination of the rich history of Al coordination chemistry and the development of non-innocent ligands has set forth a solid foundation for considerable research. In Chapter 2, novel Al complexes with a non-innocent ligand that demonstrates unique ligand-based proton-transfer are discussed. Chapter 3 introduces Al complexes with primary phosphido ligands that have the potential to support unique redox-transfer reactions.

1.6 References.

---

[1] Ludwig, J. R.; Schindler, C. S. Catalyst: Sustainable Catalysis. *Chem*. **2017**, *2*, 313-316.

[2] Sivaram, S. Organoaluminum Chemistry and Its Application to The Initiation Of Carbenium Ion Polymerization. *J. Organomet. Chem*. **1978**, *156*, 55-64.

[3] Power, P. P. Main-group Elements as Transition Metals. *Nature*. **2010**, *463*, 171-177.

[4] Weetman, C.; Inoue, S. The Road Travelled: After Main-Group Elements as Transition Metals. *ChemCatChem*. **2018**, *10*, 4213-4228.

[5] Weetman, C.; Xu, H.; Inoue, S. Recent Developments in Low-Valent Aluminum Chemistry. *Encyclopedia of Inorganic and Bioinorganic Chemistry*, Wiley: **2020;** pp 1-20.

[6] Hobson, K.; Carmalt, C. J.; Bakewell, C. Recent Advances in Low Oxidation State Aluminium Chemistry. *Chem. Sci*. **2020**, *11*, 6942– 6956.

[7] Stennett, T. E.; Pahl, J.; Zijlstra, H. S.; Seidel, F. W.; Harder, S. A Frustrated Lewis Pair Based on a Cationic Aluminum Complex and Triphenylphosphine. *Organometallics*. **2016**, *35*, 207-217.

[8] Schultz, R. F. Organoaluminum Compounds. *Advances in Chemistry*. **1959**, *23*, 163-171.

[9] Mason, M. R. Aluminum-Based Catalysis. *Encyclopedia of Inorganic and Bioinorganic Chemistry*, Wiley: **2015**; pp 1-22.

[10] Herzog, S.; Geisler, K.; Präkel, H. A Neutral Complex of Aluminum with 2,2′-Bipyridyl. *Angew. Chem. Int. Ed.* **1963**, *2*, 47-48.

[11] Bellavance, P. L.; Corey, E. R.; Corey, J. Y.; Hey, G. W. Synthesis and characterization of complexes of aluminum halide with 2,2'-bipyridine, 1,10-phenanthroline and 2,2',2"-terpyridine in acetonitrile. *Inorg. Chem.* **1977**, *16*, 462-467.

[12] Finnegan, M. M.; Rettig, S. J.; Orvig, C. Neutral water-soluble aluminum complex of neurological interest. *J. Am. Chem. Soc.* **1986**, *108*, 5033-5035.

[13] Robinson, G. H.; Sangokoya, S. A. The organometallic coordination chemistry of aluminum. Synthesis and molecular structure of $[(CH_3)Al]_2[C_8H_2ON_6][Al(CH_3)_2]_2$: a novel example of a neutral organoaluminum complex containing two five-coordinate aluminum atoms in square-pyramidal environments. *J. Am. Chem. Soc.* **1987**, *109*, 6852-6853.

[14] Liu, S.; Rettig, S. J.; Orvig, C. Polydentate ligand chemistry of Group 13 metals: effects of the size and donor selectivity of metal ions on the structures and properties of aluminum, gallium, and indium complexes with potentially heptadentate (N_4O_3) amine phenol ligands. *Inorg. Chem.* **1992**, *31*, 5400-5407.

[15] Aida, T.; Inoue, S. Activation of carbon dioxide with aluminum porphyrin and reaction with epoxide. Studies on (tetraphenylporphinato)aluminum alkoxide having a long oxyalkylene chain as the alkoxide group. *J. Am. Chem. Soc.* **1983**, *105*, 1304-1309.

[16] Darensbourg, D. J.; Maynard, E. L.; Holtcamp, M. W.; Klausmeyer, K. K.; Reibenspies, J. H. Synthesis and X-ray Structure of the Novel Aluminum Complex $[\{\eta^3\text{-HB(3-Phpz)}_2\text{(5-Phpz)}\}_2\text{Al}][\text{AlCl}_4]$. Catalysis of CO_2/Propylene Oxide to Propylene Carbonate by the $AlCl_4^-$ Anion. *Inorg. Chem.* **1996**, *35*, 2682-2684.

[17] Qian, B.; Ward, D. L.; Smith, M. R. Synthesis, Structure, and Reactivity of β-Diketiminato Aluminum Complexes. *Organometallics* **1998**, *17*, 3070-3076.

[18] Emig, N.; Nguyen, H.; Krautscheid, H.; Réau, R.; Cazaux, J.-B.; Bertrand, G. Neutral and Cationic Tetracoordinated Aluminum Complexes Featuring Tridentate Nitrogen Donors: Synthesis, Structure, and Catalytic Activity for the Ring-Opening Polymerization of Propylene Oxide and (d,l)-Lactide.

[19] Stephan, D. W. Frustrated Lewis Pairs: From Concept to Catalysis. *Acc. Chem. Res.* **2015**, *48*, 306-316.

[20] Zhang, Y.; Miyake, G. M.; Chen, E. Y.-X. Alane-Based Classical and Frustrated Lewis Pairs in Polymer Synthesis: Rapid Polymerization of MMA and Naturally Renewable Methylene Butyrolactones into High-Molecular-Weight Polymers. *Angew. Chem., Int. Ed.* **2010**, *49*, 10158-10162.

[21] Appelt, C.; Westenberg, H.; Bertini, F.; Ehlers, A. W.; Slootweg, J. C.; Lammertsma, K.; Uhl, W. Geminal Phosphorus/Aluminum-Based Frustrated Lewis Pairs: C-H versus C-C Activation and CO2 Fixation. *Angew. Chem., Int. Ed.* **2011**, *50*, 3925-3928.

[22] Bag, P.; Weetman, C.; Inoue, S. Experimental Realisation of Elusive Multiple-Bonded Aluminium Compounds: A New Horizon in Aluminium Chemistry. *Angew. Chem., Int. Ed.* **2018**, *57*, 14394-14413.

[23] Dohmeier, C.; Robl, C.; Tacke, M.; Schnöckel, H. The Tetrameric Aluminum(I) Compound [{Al(η^5-C_5Me_5)}$_4$]. *Angew. Chem., Int. Ed.* **1991**, *30*, 564-565.

[24] Cui, C.; Roesky, H. W.; Schmidt, H.-G.; Noltemeyer, M.; Hao, H.; Cimpoesu, F. Synthesis and Structure of a Monomeric Aluminum(I) Compound [{HC(CMeNAr)$_2$}Al] (Ar=2,6–*i*Pr$_2$C$_6$H$_3$): A Stable Aluminum Analogue of a Carbene. *Angew. Chem., Int. Ed.* **2000**, *39*, 4274-4276.

[25] Zhong, M.; Sinhababu, S.; Roesky, H. W. The unique β-diketiminate ligand in aluminum(I) and gallium(I) chemistry. *Dalton Trans.* **2020**, *49*, 1351-1364.

[26] Hicks, J.; Vasko, P.; Goicoechea, J. M.; Aldridge, S. Synthesis, structure and reaction chemistry of a nucleophilic aluminyl anion. *Nature* **2018**, *557*, 92-95.

[27] Hicks, J.; Vasko, P.; Goicoechea, J. M.; Aldridge, S. Reversible, Room-Temperature C—C Bond Activation of Benzene by an Isolable Metal Complex. *J. Am. Chem. Soc.* **2019**, *141*, 11000-11003.

[28] Schwamm, R. J.; Anker, M. D.; Lein, M.; Coles, M. P. Reduction vs. Addition: The Reaction of an Aluminyl Anion with 1,3,5,7-Cyclooctatetraene. *Angew. Chem., Int. Ed.* **2019**, *58*, 1489-1493.

[29] Schwamm, R. J.; Coles, M. P.; Hill, M. S.; Mahon, M. F.; McMullin, C. L.; Rajabi, N. A.; Wilson, A. S. S. A Stable Calcium Alumanyl. *Angew. Chem., Int. Ed.* **2020**, *59*, 3928-3932.

[30] Kurumada, S.; Takamori, S.; Yamashita, M. An alkyl-substituted aluminium anion with strong basicity and nucleophilicity. *Nat. Chem.* **2020**, *12*, 36-39.

[31] Koshino, K.; Kinjo, R. Construction of σ-Aromatic AlB2 Ring via Borane Coupling with a Dicoordinate Cyclic (Alkyl)(Amino)Aluminyl Anion. *J. Am. Chem. Soc.* **2020**, *142*, 9057-9062.

[32] Schrauzer, G. N.; Mayweg, V. Reaction of Diphenylacetylene with Nickel Sulfides. *J. Am. Chem. Soc.* **1962**, *84*, 3221-3221.

[33] Eisenberg, R.; Gray, H. B. Noninnocence in Metal Complexes: A Dithiolene Dawn. *Inorg. Chem.* **2011**, *50*, 9741-9751.

[34] Lyaskovskyy, V.; de Bruin, B. Redox Non-Innocent Ligands: Versatile New Tools to Control Catalytic Reactions. *ACS Catalysis* **2012**, *2*, 270-279.

[35] Chirik, P. J.; Wieghardt, K. Radical Ligands Confer Nobility on Base-Metal Catalysts. *Science* **2010**, *327*, 794-795.

[36] Bouwkamp, M. W.; Bowman, A. C.; Lobkovsky, E.; Chirik, P. J. Iron-Catalyzed [2π + 2π] Cycloaddition of α,ω-Dienes: The Importance of Redox-Active Supporting Ligands. *J. Am. Chem. Soc.* **2006**, *128*, 13340-13341.

[37] Kaim, W.; Schwederski, B. Non-innocent ligands in bioinorganic chemistry—An overview. *Coor. Chem. Rev.* **2010**, *254*, 1580-1588.

[38] Cramer, C. J.; Tolman, W. B. Mononuclear Cu–O_2 Complexes: Geometries, Spectroscopic Properties, Electronic Structures, and Reactivity. *Acc. Chem. Res.* **2007**, *40*, 601-608.

---

[39] Himo, F.; Eriksson, L. A.; Maseras, F.; Siegbahn, P. E. M. Catalytic Mechanism of Galactose Oxidase: A Theoretical Study. *J. Am. Chem. Soc.* **2000**, *122*, 8031-8036.

[40] Whittaker, J. W., Galactose oxidase. *Adv. Protein Chem*. **2002**, *60*, 1-49.

[41] Wang, Y.; Stack, T. D. P. Galactose Oxidase Model Complexes: Catalytic Reactivities. *J. Am. Chem. Soc.* **1996**, *118*, 13097-13098.

[42] Sherbow, T. J.; Parsons, L. W. T.; Phan, N. A.; Fettinger, J. C.; Berben, L. A. Ligand Conjugation Directs the Formation of a 1,3-Dihydropyridinate Regioisomer. *Inorg. Chem.* **2020**, *59*, 17614-17619.

Chapter 2: A Bis(enol)amine Ligand Protonation Series of Aluminum(III) Complexes

2.1 Introduction.

The most common coordination mode for the ONO ligand (1,1'-azanediylbis(3,3-dimethylbutan-2-one) is as ONO^{3-}, where triple deprotonation has been affected. As examples, complexes of P(III), P(V),[1] As(III),[2] and Sb(III), have been reported with various ancillary ligands to fill out their coordination sphere. Redox chemistry associated with ONO^{3-} is generally oxidative and can either involve the ONO^{3-} fragment or the central ion of a complex, and this of course depends on their relative oxidation potentials. As an example, in the case of P(III) in $(ONO^{3-})P^{III}$, oxidation to a series of $(ONO^{3-})P^{V}X_2$ complexes, where X includes H^-, NHPh, or NH_2, has been documented.[3,4,5,6] Analogous to the P(III/V) examples, single reports of As(III/V) and Sb(III/V) interconversion, have been reported where the ligand remains as ONO^{3-} throughout the redox processes. [7,8,9]

Complexes of the oxidized ligand, ONO^- have also been reported, and these are generally observed when electron transfer occurs concomitant with ligand coordination to the central ion. Coordination of ONO^- to Si(II), Ge(II), and Sn(II) has been observed in reactions of Si(IV), Ge(IV), and Sn(IV) precursors,[10] respectively, with the deprotonated ONO^{3-}. As an example, synthesis of the Si(II)-containing dimer $([ONO^-]SiR)_2$ was performed starting with Si(IV) reagents, $RSiCl_3$, where R = H, Ph, Cl, Br.[11] Synthesis of $(ONO^-)_3Bi$ was achieved from $BiCl_3$ and ONO^{3-} although the source of six oxidizing equivalents was not identified in that case.[12]

The $(ONO^{3-})Pn$ scaffold, where Pn = pnictogen, has also been isolated as an adduct with various transition metal complexes where the lone pair on the pnictogen can coordinate to a metal as a neutral donor ligand. A series of complexes of $(ONO^{3-})P$ coordinated to Pt,[13] Ag,[14] Mn,[15] Ru,[16] Fe, Cr, W, Ni, and Pd,[17] have been characterized. Similarly, the analogous $(ONO^{3-})As$ and $(ONO^{3-})Sb$ scaffold also form adducts with transition metals.[13-17]

Efforts to probe a range of protonation states on ONO have not been extensively discussed in the literature and we therefore cannot determine to what extent this chemistry has been explored. As an example report, reaction of $(\eta^3\text{-}ONO^{3-})P$ with HOTf or MeOH affords $[(\eta^2\text{-}ONO^{2-})P]OTf$ (**A**) or $(\eta^2\text{-}ONO^{2-})P(OMe)$ (**B**), respectively, and in each molecule the $HONO^{2-}$ ligand is asymmetric and protonated at one of the carbon atoms adjacent to the *N*-donor. One of the *O*-donors dissociated from the P(III) center, and protonation was not shown to be reversible (Scheme 1).[8] Reaction of the P(V) complex $(\eta^3\text{-}ONO^{3-})PCl_2$ with TASF (tris(dimethylamino)sulfonium difluorosiliconate) gave $(\eta^3\text{-}HONO^{2-})PF_3$ (**C**).[8] Again, the resulting $\eta^3\text{-}HONO^{2-}$ is asymmetric, protonated at one of the C atoms and neither further deprotonation nor re-protonation chemistry was discussed. Partial deprotonation chemistry has also been initiated beginning at the H_3ONO ligand before coordination to a metalloid. In both of those examples, the asymmetric ligand was observed in $[(\eta^2\text{-}HONO^{2-})E]_2$, where E = Ge(IV), or Sn(IV) (**D**), and further deportation or re-protonation efforts were not explicitly described.[9]

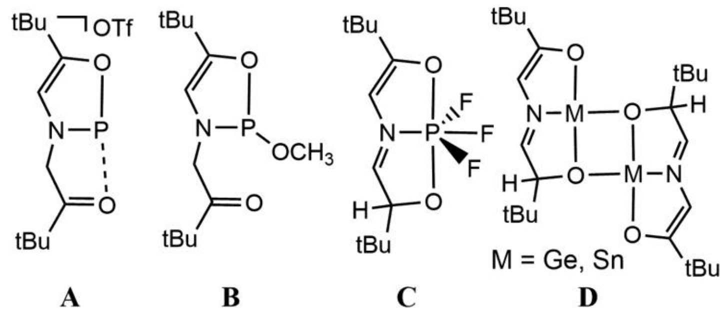

Scheme 2.1. Summary of previous reports on protonation chemistry of ONO^{3-} (in each complex the ligand is $HONO^{2-}$)

In this work we explore the effect on ONO ligand chemistry of employing highly electrophilic central ion such as Al(III), which might form stronger ionic interactions with ONO to stabilize the lower-charged $HONO^{2-}$ and H_2ONO^{-} complexes to enable interconversion between protonation states. Recent work on the chemistry of non-innocent ligands has demonstrated that both electron transfer *and* proton transfer can often be accessed in combination with a suitable central supporting ion.[18] To determine whether additional protonation states of ONO could be accessed in this report, we employed Al(III). The stability of Al(III) to both oxidation and reduction makes it ideal to support a wide range of charge and protonation states as has been demonstrated using ligands such as iminopyridine,[19] di(imino)pyridines,[20] α-diimines,[21] dpp-BIAN,[22] bis(pyrazolyl)pyridine,[18b] and amidobis(phenolate).[23] Here Al(III) enables us to introduce two additional electronic structures for the protonation states of ONO: $HONO^{2-}$ and H_2ONO^{-}, along with interconversion of these compounds in acid-base reactions (Scheme 2.2). However, the ubiquitous ONO^{3-} protonation state is not accessible. We also explore the ligand-based oxidation and reduction chemistry using cyclic voltammetry, and the reaction chemistry of the $HONO^{2-}$ and H_2ONO^{-} complexes.

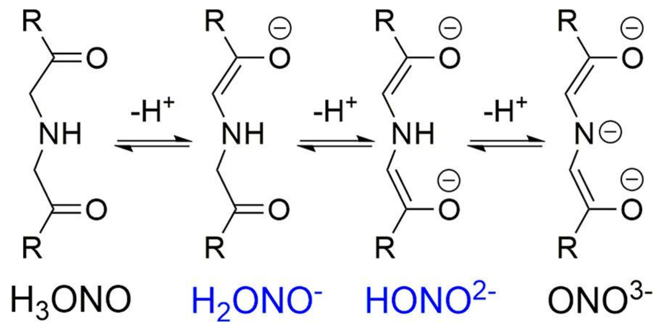

Scheme 2.2. Possible protonation states of ONO (blue labels denote protonation states in this work; R = ^{t}Bu)

2.2 Results and Discussion.

2.2.1. Synthesis of Compounds. Synthesis of Al complexes containing the ONO ligand have been achieved by deprotonating H_3ONO with potassium hydride (KH). Deprotonation of H_3ONO with 1 equivalent of KH, followed by the addition of $AlCl_3$ in THF resulted in formation of the orange compound which was identified as a pseudo-octahedral complex, $[(H_2ONO^-)_2Al][AlCl_4]$ (**2.1**), in which the two ligands are each deprotonated once (Scheme 2.3). The site of deprotonation at one of the α-carbons is evident in the ^{1}H NMR spectroscopic measurements which are consistent with an asymmetric electronic structure for H_2ONO^- (Figure 2.1). The methylene and vinylic protons flanking the amine appear with three distinct chemical shifts. The vinylic proton is a doublet at 4.78 ppm (J_{HH} = 5.1 Hz), one methylene proton appears as a doublet of doublets (3.97 ppm, J_{HH} = 19.1 and 5.1 Hz), and the other methylene proton appears as a doublet at 3.76 ppm (J_{HH} = 19.1 Hz). The vinylic proton and the first methylene proton are split by the N—H proton, which appears as a singlet resonance at 5.18 ppm, and the methylene protons split each other. The IR spectrum shows an N—H stretch at 3264 cm^{-1}, a C=O band at 1657 cm^{-1} and a C—O band at 1095 cm^{-1}.

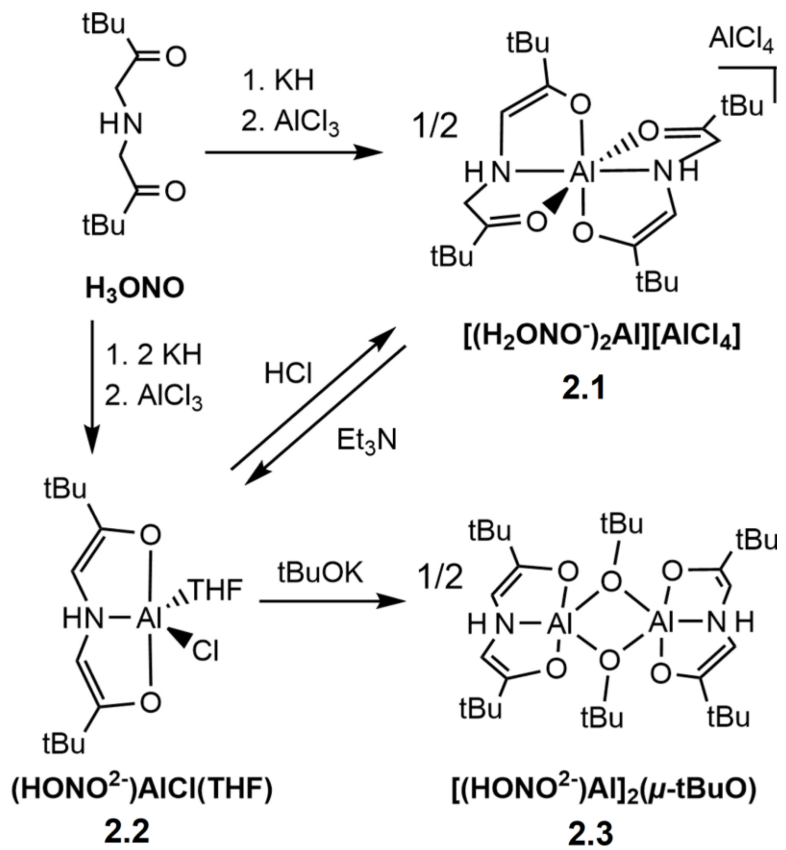

Scheme 2.3. Synthesis of **2.1, 2.2,** and **2.3**

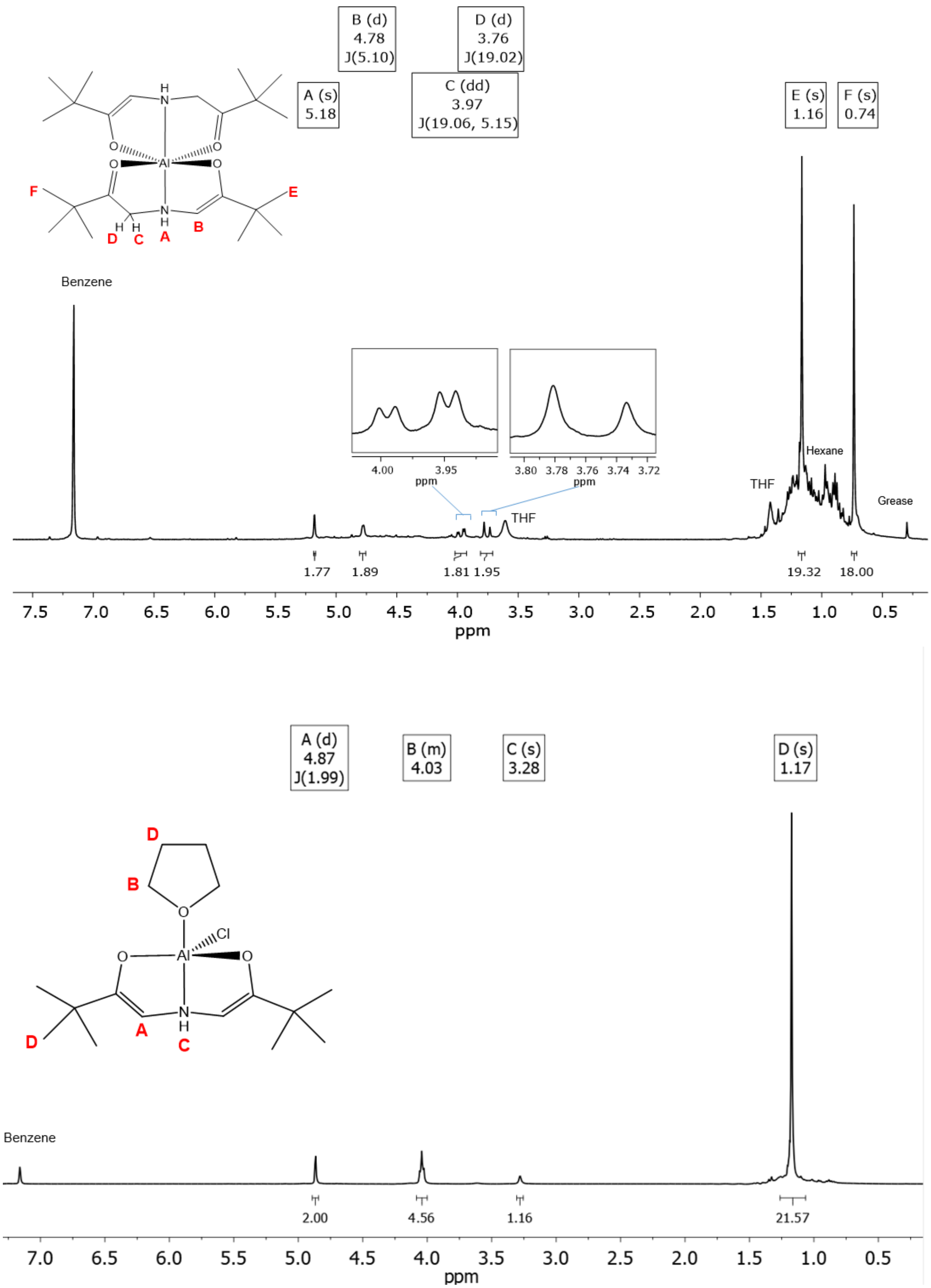

Figure 2.1. ^{1}H NMR spectrum of **2.1** (top) and **2.2** (bottom).

Reaction between H_3ONO and 2 equivalents of KH over two hours was followed by addition of $AlCl_3$ in THF, and gave a purple-colored solution. Upon workup, a five-coordinate pseudo-trigonal bipyramidal complex ($HONO^{2-}$)AlCl(THF) (**2.2**), was isolated in 70% yield (Scheme 2.3). Both α-carbon positions are deprotonated, and the ligand appears symmetric when probed by ^1H NMR spectroscopy (Figure 2.1). The vinylic C—H resonance is observed at 4.87 ppm as a doublet (J_{HH} = 1.99 Hz), and the N—H resonance appears as singlet at 3.28 ppm. The IR spectrum shows an N—H stretch at 3271 cm^{-1}, the sp^2 C-H absorption band at 3098 cm^{-1}, and a CO band at 1108 cm^{-1}. To probe the potential for exchange of ligand H atoms, the NMR spectra of complexes **2.1** and **2.2** were recorded on solutions exposed to D_2 for 24 h. No evidence for exchange was observed.

The ONO^{3-} charge state has been observed in many previous reports and in an attempt to obtain an Al complex with ONO^{3-}, reaction between H_3ONO and 3 equivalents of KH over two hours was followed by addition of $AlCl_3$ dissolved in THF. A mixture of unidentifiable products was observed using proton NMR spectroscopy. Deprotonation of **2.2** was also explored in efforts to isolate Al(III) complexes containing fully deprotonated ONO^{3-}. Reaction of **2.2** with KH or Et_3N afforded no change to **2.2**. Reaction of **2.2** with *n*BuLi yielded a color change from purple to pale yellow, but the resulting ^1H NMR spectrum contained large numbers of resonances in the alkyl region which suggested multiple products and decomposition. Reaction of **2.2** with ^tBuOK yielded the dimeric complex $[(HONO^{2-})Al]_2(\mu\text{-}^tBuO)_2$ (**2.3**), in which the $HONO^{2-}$ ligand in **2.2** has not been deprotonated, but KCl has been eliminated as byproduct to yield an Al_2O_2 diamond core structure (Scheme 2.3, Figure 2.2).

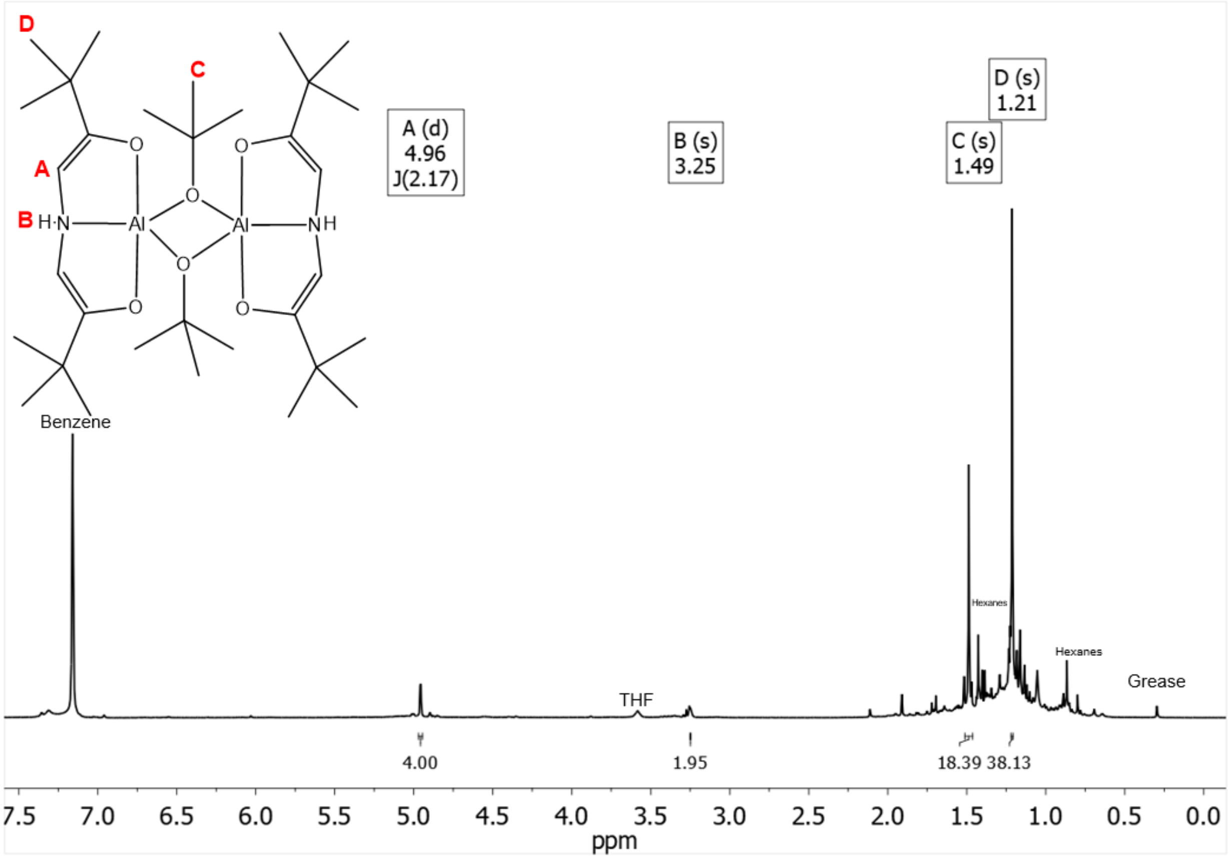

Figure 2.2. ^{1}H-NMR spectrum of [(HONO^{2-})Al](μ-tBuO) (**2.3**)

In a series of reactions, we explored the possibility of accessing a protonation series with either one ligand per Al center, as in **2.2**, or with two ligands per Al center, as in **2.1**. Reaction of **2.1** with one equivalent of Et_3N successfully deprotonated H_2ONO^- to $HONO^{2-}$, but rearrangement of the metal-ligand connectivity afforded **2.2** in 52% yield. We reasoned that exchange of the $[AlCl_4]^-$ counteranion in **2.1** with anions such as PF_6^- or $CF_3SO_3^-$ may prevent formation of **2.2**, however reaction of both $NaPF_6$ and $NaCF_3SO_3$ with **1.2** afforded intractable mixtures. Complex **2.2** can be selectively protonated at just one of the α-enolate carbon atoms in a reaction with one equivalent of HCl dissolved in ether. In that reaction, rearrangement of metal-ligand connectivity also occurs so that the bis(ligand) complex **2.1** was obtained in 42%

yield (Scheme 2.3). The same reactivity was observed with weaker acids such as [HDMAP][BF_4] (pK_a = 13.6 in THF,[24] Figure 2.3). Thus far, we have been unable to generate a protonation series with a single ligand bound to the Al center.

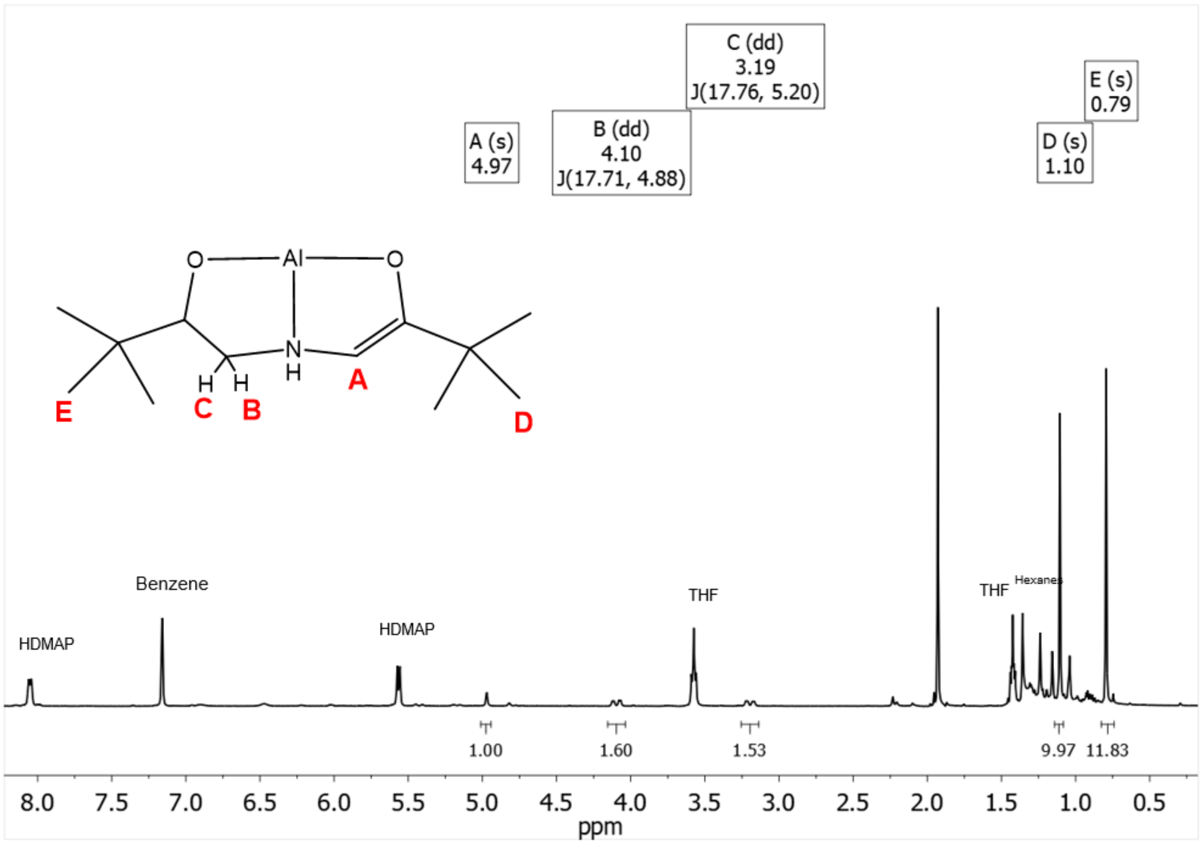

Figure 2.3. ^{1}H-NMR spectrum of ($HONO^{2-}$)AlCl(THF) with one equivalent of [HDMAP][BF_4].

The resistance of **2.2** toward deprotonation led us to explore the effects of providing additional donating ligands to the Al(III) center to potentially stabilize the ONO^{3-} protonation state. We explored reaction of **2.2** with bidentate ligands oxalate, bipyridine, and 2,4-di-^{t}butylcatecholate, but detected no reaction in each case. The reaction of **2.2** with two equivalents of monodentate 2,2,6,6-tetramethylpiperidine-*N*-oxyl (TEMPO) afforded [($HONO^{2-}$

)Al(TEMPO)(TEMPOH)] (**2.4**) in 84% yield (Scheme 2.4). The protonation state of the HONO^{2-} ligand is unchanged in the product as compared with the reactant.

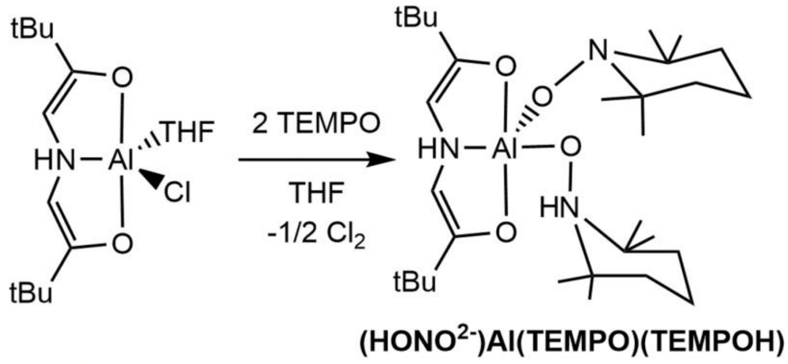

Scheme 2.4. Synthesis of [(HONO^{2-})Al(TEMPO)(TEMPOH)] (**2.4**)

The ^{1}H NMR spectrum of **2.4** supports the ligand assignment as symmetric with protonated *N*-donor atom (Figure 2.4): a vinylic C-H resonance is observed at 6.85 ppm as a singlet, and the protonated HONO^{2-} N-H resonance at 9.51 ppm in proton NMR spectra. Two TEMPO ligands coordinate the Al center and one of those appears to be protonated. In the proton NMR spectrum the TEMPOH N-H resonance appears at 6.53 ppm. Previous reports of TEMPO protonated at the N-H position include complexes of B,[25] Ni,[26] Zr,[27] and Ir,[28] and those TEMPOH N-H resonances were observed at 7.25, 7.62, 7.36, and 12.32 ppm, respectively. Broad IR absorption bands appear at 3403 and 3255, and are reasonably attributed to the N-H bonds in HONO^{2-} and in TEMPOH, respectively.

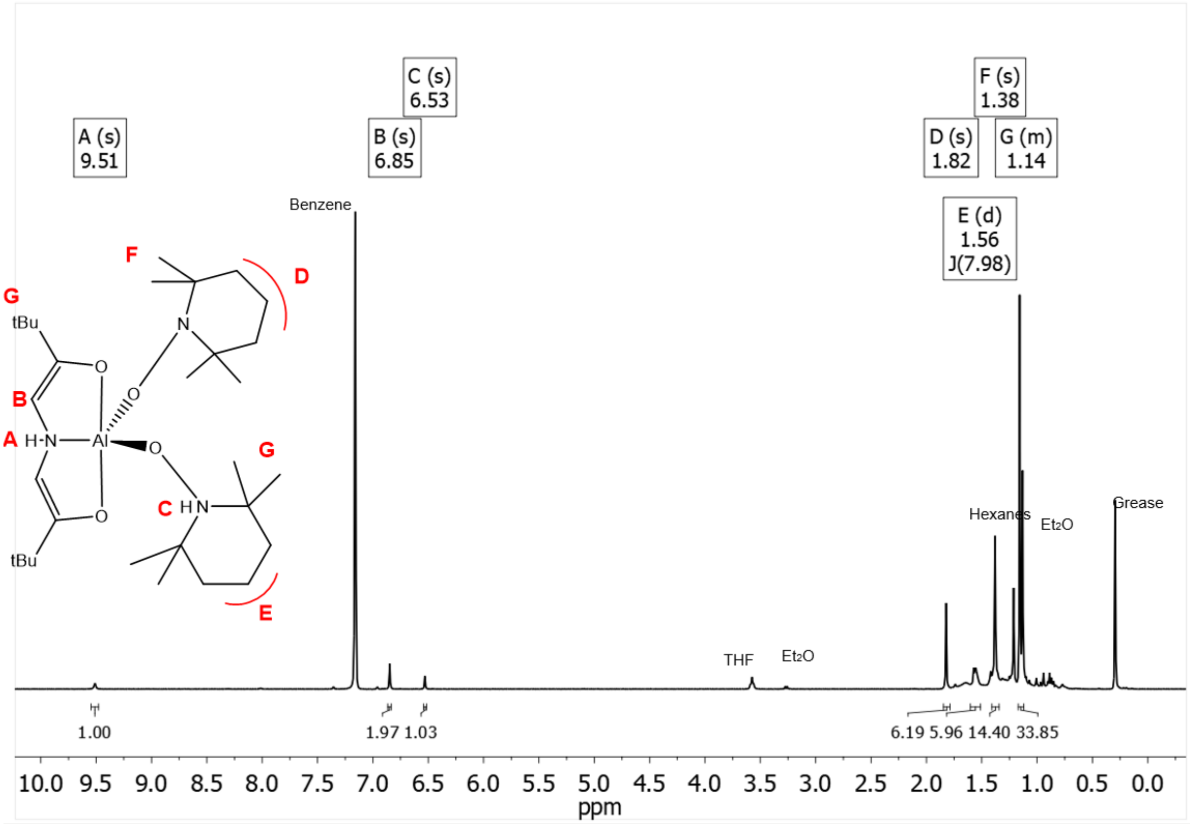

Figure 2.4. ^{1}H-NMR spectrum of (HONO^{2-})Al(TEMPO)(TEMPOH) (**2.4**)

We also attempted to elucidate details of the mechanism for formation of **2.4** which contains both an anionic η^1-TEMPO ligand and a neutral, protonated η^1-TEMPOH ligand coordinated to the Al center (Scheme 2.4). Formally, each TEMPO radical has been reduced by one electron in **2.4** but the charge state of the ONO ligand remains unchanged between reactant and product. We propose that reduction of TEMPO may be coupled with the oxidation and dissociation of the chloro ligand which is not present in **2.4**. TEMPO is a strong oxidizing agent ($E°$ = 1.24 V vs. SCE),[29] and Cl^- is oxidized at 1.12 V vs. SCE,[30] so it is possible that the chloro ligand is oxidized to Cl_2, and this would provide one electron toward the observed two-electron reduction. Indeed, the reaction solutions are initially green-brown in color and become brown upon exposure to vaccum which may suggest the formation of chlorine gas. The synthesis of **2.4** was repeated in the presence of the olefins cyclohexene, 9,10-dihydroanthracene, and styrene in an attempt to isolate chlorinated products however none were detected by proton NMR spectroscopy or GC-MS. The unreacted olefins were observed in those spectra.

We further reasoned that formation of protonated TEMPOH may occur by abstraction of $H^{\bullet}$ from THF solvent: the reaction yield of **2.4** is consistently 65 - 84% and so it is unlikely that $H^{\bullet}$ is derived from ligand decomposition. A $H^{\bullet}$ transfer would also account for the second electron. Protonated TEMPO Al complexes have been previously observed by Hayton and co-workers,[31] and in those examples the proton is derived either from the oxidation of alcohols or from 9,10-dihydroanthracene. Accordingly, reaction of **2.2** with 2 equivalents of TEMPO was performed in d_8-THF and the product was interrogated using ^{1}H-NMR spectroscopy (Figure 2.5). No deuterated products were detected. We also prepared d_8-**2** using d_8-THF as solvent so that the solvate THF molecule is deuterated (Figure 2.6). The reaction of d_8-**2.2** with 2 equivalents of TEMPO was performed in d_6-benzene and the ^{1}H-NMR spectrum revealed the loss of the N—H resonance at 6.53 ppm (Figure 2.5). The reaction suggests that in the synthesis of **2.4,** TEMPO is protonated via $H^{\bullet}$ abstraction from the solvate THF molecule in an intramolecular process. The reaction of **2.2** with 2 equivalents of TEMPO was also performed in d_6-benzene and the ^{1}H-NMR spectrum revealed no deuterium incorporation (Figure 2.5).

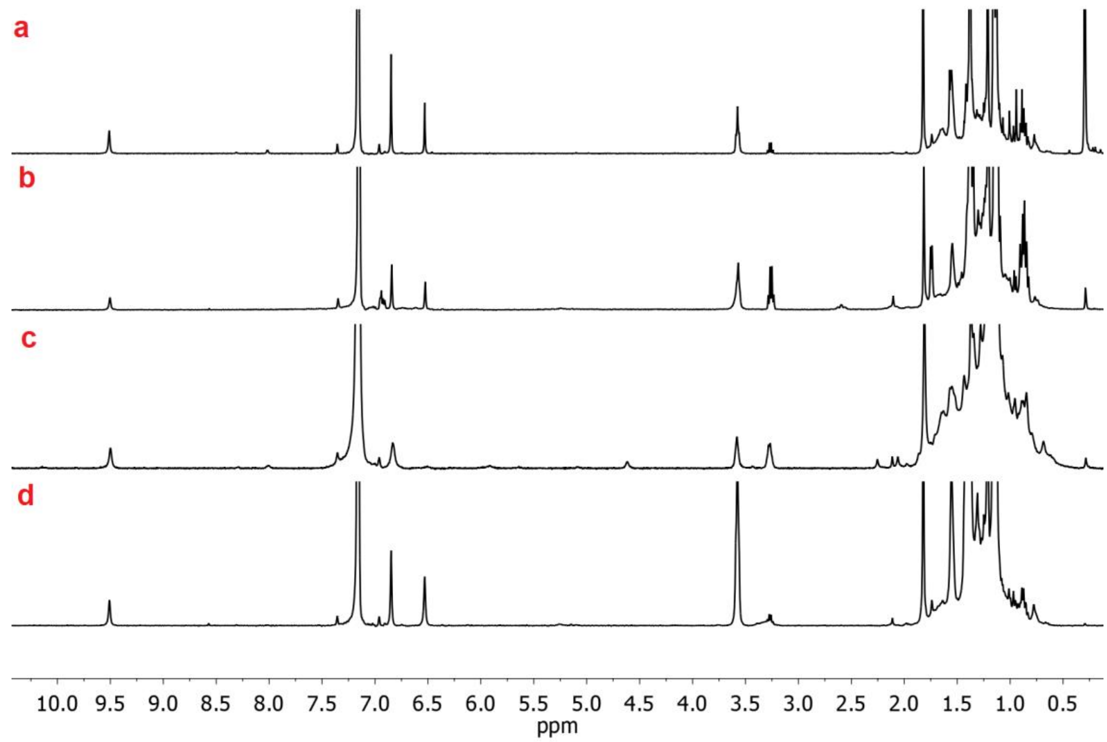

Figure 2.5. ^{1}H NMR spectra for: a) (HONO^{2-})Al(TEMPO)(TEMPOH) (**2.4**) synthesized in THF from **2.2**; b) **2.4** synthesized in d_8-THF from **2.2**; c) d_1-**2.4** synthesized from d_8-**2.2** in C_6D_6; and d) **2.4** synthesized from **2** in C_6D_6. Assignments for the peaks are given in Figure 2.4.

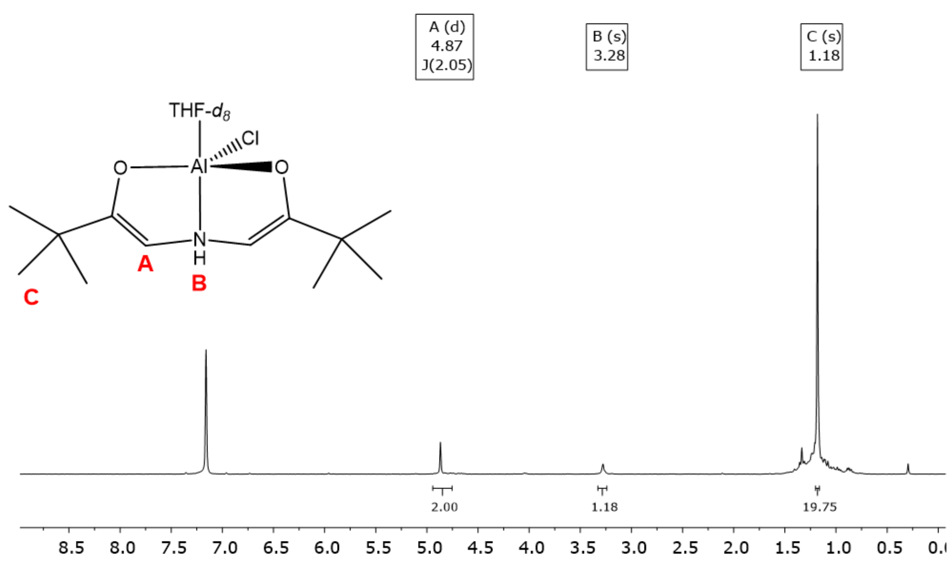

Figure 2.6. ^{1}H-NMR spectrum of (HONO^{2-})AlCl(d_8-THF) (d_8-**2.2**).

2.2.2. Solid State Structures. Single crystals of **2.1** were grown as pale orange plates from a concentrated toluene solution held at -15 °C overnight (Figure 2.1, Table 2.1, and Table 2.2). The solid-state structure of **2.1** was characterized by single-crystal X-ray diffraction. The bond lengths and angles in **2.1** suggest that the H_2ONO^- ligand is deprotonated once at an α-carbon position and is monoanionic. The anionic ligand charge appears localized on one enolate *O*-donor, where the Al-O bond length is 1.836(3) Å and the C-O bond length is 1.315(5) Å. The other Al-O and C-O bonds in **2.1** are 1.978(3) Å, and 1.209(5) Å, respectively.

	1	**2**	**3**	$(ONO^{3-})PH_2$ [4]
M—O	1.836(3)	1.773(10)	1.7749(9)	1.721(1)
	1.978(3)	1.7745(10)		1.699(2)
M—N	2.006(4)	2.0592(10)	2.1210(15)	1.676(2)
C—O	1.315(5)	1.3624(15)	1.3468(15)	1.384(2)
	1.209(5)	1.3450(15)		
C—N	1.456(5)	1.4665(15)	1.4591(18)	1.400(2)
	1.494(5)	1.4641(15)		
C—C	1.347(6)	1.3456(18)	1.332(2)	1.325(2)
	1.513(6)	1.3438(17)		

Table 2.1 Select average bond distances for **2.1**, **2.2**, and **2.3**.

	1[a]	**2**[b]	**3**[b]	**4**[b]
Formula	$C_{31}H_{52}Al_2Cl_4N_2O_4$	$C_{16}H_{29}AlClNO_3$	$C_{32}H_{60}Al_2N_2O_6$	$C_{30}H_{39}AlN_3O_4$
Crystal size	0.28 × 0.19 × 0.18	0.89 × 0.54 × 0.48	0.26 × 0.18 × 0.17	0.41 × 0.27 × 0.26
Formula weight, g mol^{-1}	237.50	345.83	622.78	532.63
Space group	$P\bar{1}$	$P2_12_12_1$	$C2/m$	$P2_1/c$
a, Å	11.2959(4)	10.1142(10)	13.6133(5)	12.2305(3)
b, Å	19.5809(7)	10.4277(10)	18.4236(6)	12.0552(3)
c, Å	19.6873(8)	18.2304(17)	9.7708(3)	22.6611(6)
α, deg	113.942(2)	90	90	90
β, deg	94.859(2)	90	94.3910(12)	96.8336(11)
γ, deg	93.987(2)	90	90	90
V, Å^3	3939.6(3)	1922.7(3)	2443.38(14)	3317.44(15)
Z	4	4	2	4
T, K	100(2)	90(2)	100(2)	90(2)
ρ, calcd, g cm^{-3}	1.201	1.195	0.846	1.105
Refl. collected/$2\theta_{max}$	28951/140.726	21879/61.138	8551/144.756	20429/144.828
Unique refl./ $I > 2\sigma(I)$	14974/11456	5864/5706	2496/2236	6458/6108
No. parameters/restraints	975/216	209/0	130/0	421/0
λ, Å / μ (Kα), cm^{-1}	1.54178	0.71073	1.54178	1.54178
R_1/GOF	0.0775/1.059	0.0276/1.0004	0.0376/1.066	0.0461/1.1.35
$wR_2(I > 2\sigma(I))^c$	0.2176	0.0706	0.0987	0.1257
Residual density, e Å^{-3}	1.036/-0.607	0.593/-0.183	0.200/-0.214	0.509/-0.241

[a]Obtained with graphite-monochromated Mo Kα (λ = 0.71073 Å) radiation. [b]Obtained with graphite-monochromated Cu Kα (λ = 1.54178 Å) radiation. [c]$R_1 = \Sigma||F_o|-F_c||/\Sigma|F_o|$, $wR_2 = \{\Sigma[w(F_o{}^2-F_c{}^2)^2]/ \Sigma [w(F_o{}^2)^2]\}^{1/2}$.

Table 2.2. Crystollographic data for $[(H_2ONO^-)_2Al][AlCl_4]$ (**2.1**), $(HONO^{2-})AlCl(THF)$ (**2.2**), $[(HONO^{2-})Al]_2(\mu\text{-}^tBuO)_2$ (**2.3**), and $(HONO^{2-})Al(TEMPO)(TEMPOH)$ (**2.4**).

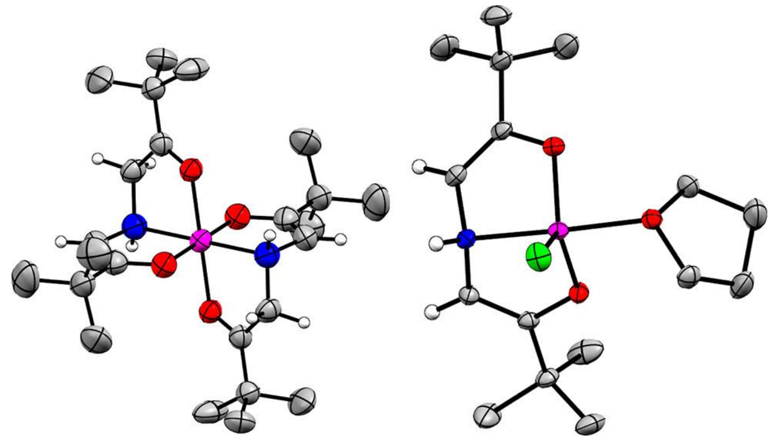

Figure 2.7. Solid state structures of (left) $[(H_2ONO^-)_2Al]^+$ in **2.1**, and (right) ($HONO^{2-}$)AlCl(THF) in **2.2**. Pink, red, blue, gray, green and white represent Al, O, N, C, Cl and H atoms, respectively. Thermal ellipsoids at 50% probability. *t*-Bu H atoms omitted.

Single crystals of **2.2** suitable for X-ray diffraction were grown as pale purple plates from a concentrated solution of 1:1 hexanes/toluene held at -15 °C overnight (Figure 2.7, Table 2.1, Table 2.2). Based on the Al-ligand bond angles, we calculated the τ_5 value for **2.1** as 0.70, and this indicates that the Al center is best described as pseudo-trigonal pyramidal in geometry.[32] The bond lengths for **2** suggest that the ligand framework is symmetric and that both α-carbon positions are deprotonated. The ligand is dianionic as evidenced by the elongated C—O bonds, 1.3624(15) and 1.3540(15) Å, and the shortened Al—O bonds 1.7723(10) and 1.745(1) Å. Despite the higher overall anionic ligand charge in **2.2**, relative to **2.1**, the Al—N bond length is approximately the same, at 2.0592(10) compared with 2.006(4) Å.

Single crystals of **2.3** were grown as blue blocks from a concentrated toluene solution held at -15 °C overnight (Figure 2.8, Table 2.1, and Table 2.2). The Al—O and C—O bond lengths in **2.3** are very similar to those in **2.2**, at 1.7749(9) and 1.3468(15) Å, respectively, and these comparisons suggest that the best assignment for **2.3** is with $HONO^{2-}$, in agreement with spectroscopic data. Single crystals of **2.4** were grown as blue needles from a concentrated solution of 1:1 hexanes/toluene held at 15 °C overnight. The τ_5 value of **2.4** is 0.72, consistent with a pseudo-trigonal pyramidal geometry.[32] The average Al-O and C-O bond lengths in **2.4** are similar to those in **2.2**, at 1.8200(11) Å and 1.3486(19) Å, respectively. These metrics, along with the proton NMR and IR data confirm that the ligand is best described as being in the $HONO^{2-}$ charge state.

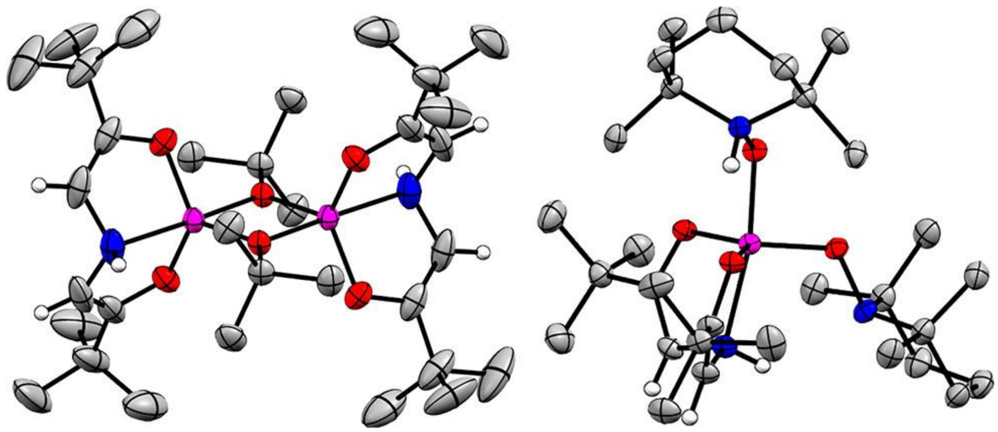

Figure 2.8. Solid state structures of (left) $[(HONO^{2-})Al]_2(\mu\text{-}^t BuO)_2$ in **2.3**, and (right) $(HONO^{2-})Al(TEMPO)(TEMPOH)$ in **2.4**. Pink, red, blue, gray, and white represent Al, O, N, C, and H atoms, respectively. Thermal ellipsoids at 50% probability. *t*-Bu H atoms and TEMPO C-H atoms omitted.

2.2.3. Electrochemical Studies. Electrochemical measurements were performed using cyclic voltammetry (CV) of complexes **2.1** and **2.2** in solutions of 0.3 M Bu_4NPF_6 THF solution (Figure 2.9).

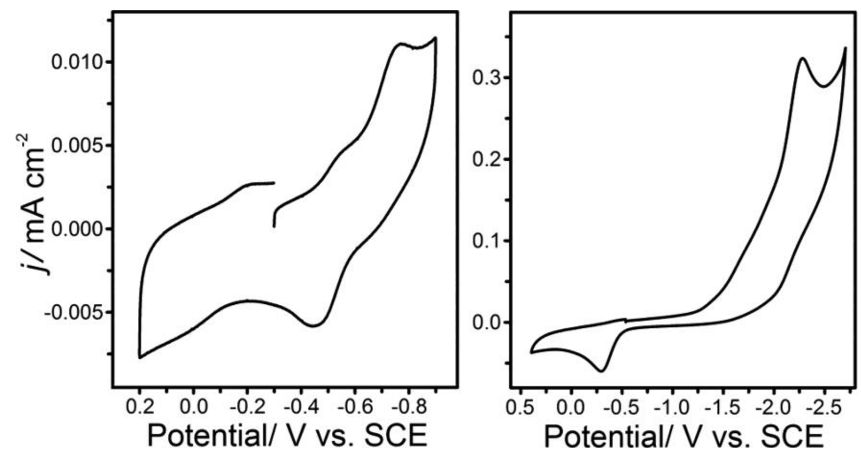

Figure 2.9. Cyclic voltammograms of 0.5 mM **2.1** (left) and 1 mM **2.2** (right) in 0.3 M Bu_4NPF_6 THF. Scan rate = 100 mV s^{-1}, glassy carbon working electrode.recorded in C_6H_6. Discontinuities at 950 and 1120 nm are associated with lamp and detector changes in the instrument.

The CV of **2.1** has two quasi-reversible couples that we assigned as ligand-based reduction events. The first couple occurs at -0.14 V vs. SCE, and we assign this as $H_2ONO^{0/-}$ (Scheme 2.5). The second couple was observed at -0.51 V and we assigned that as $H_2ONO^{-/2-}$. One further irreversible reduction event was observed with E_p = -0.76 V. No further processes were observed when the CV was scanned in the anodic direction. As might be expected, reduction of **2.2** which has only one proton, occurs at more negative potential than the reduction of **2.1**. The CV of **2.2** shows one irreversible reduction event with E_p = -2.26 V, and we assign this to the $HONO^{2-/3-}$ couple in **2.2**. Loss of Cl^- from the Al center, or loss of $H^\bullet$ from the ligand upon reduction could account for the irreversibility of the event at -2.26 V. There is an irreversible oxidation event at E_p = -0.32 V which we attribute to oxidation of $HONO^{2-}$ into $HONO^-$. This event persists when the CV is scanned in the anodic direction first. Chemical oxidation of **2.2** was attempted using ferrocenium hexafluorophosphate and that reaction resulted in the loss $HONO^{2-}$ ligand from Al(III).

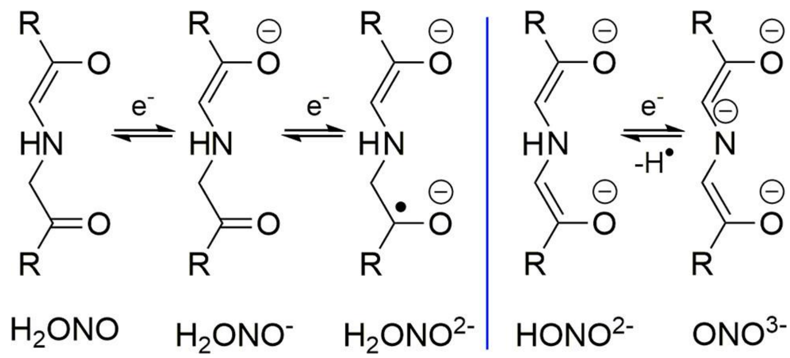

Scheme 2.5. Potentially accessible charge states of the H_2ONO (left) and HONO (right) ligands.

2.3 Conclusion.

The combination of the ONO ligand platform with highly electrophilic Al(III) has allowed the isolation of ONO ligand protonation states $HONO^{2-}$ and H_2ONO^-, along with their interconversion using Brønsted bases and acids. The substitution of ancillary chloro ligands in the $HONO^{2-}$ complex, **2.2** with oxo donors such as TEMPO and μ^2-O^{t}Bu is reported. Structural characterization of each of the reported compounds shows that the H_2ONO^- is deprotonated at one of the alpha C atoms to provide an asymmetric ligand form with unequal C-O, and C-C bond lengths. The ligand form $HONO^{2-}$ is symmetric and deprotonated twice at equivalent C atoms. Previous explorations of the chemistry of the ONO ligand have revealed numerous reports of the ONO^{3-} and the oxidized ONO^- forms, and this work has expanded on the available ligand protonation chemistry to demonstrate once again the unique influence of highly electrophilic Al(III) on ligand-based proton and electron transfer chemistry.

2.4 Experimental section.

2.4.1 Physical Measurements. Elemental analyses were performed by the Microanalytical Laboratory at The University of California, Berkeley. ^{1}H and ^{13}C NMR spectra were recorded at ambient temperature using a Varian 600 MHz or Bruker 400 MHz spectrometer.

Chemical shifts were referenced to residual solvent. Infrared spectra were recorded on a Bruker Alpha Infrared spectrometer (2 cm^{-1} resolution). GC-MS measurements were conducted on an Agilent 6890N GC with a 5973N MS. UV-Vis spectra were recorded in THF solution using an Agilent 8453 UV-Vis spectrophotometer.

2.4.2. Electrochemical Measurements. Cyclic voltammograms were recorded in a nitrogen-filled glovebox. A CH Instruments model 620D electrochemical analyzer with a glassy carbon working electrode (CH Instruments, nominal surface area of 0.071 cm^2), a platinum wire auxiliary electrode, and a $Ag/AgNO_3$ (0.001M) nonaqueous reference electrode with a Vycor tip was used. All potentials are referenced to the SCE couple, and ferrocene was used as an internal standard, where the $E_{1/2}$ value of ferrocene/ferrocenium is +0.56 V versus SCE in 0.3 M Bu_4NPF_6 THF solution.[33] Bu_4NPF_6 was recrystallized from ethanol and placed under vacuum for 72 h before electrolyte solutions were made. Electrolyte solutions were stored over 3 Å molecular sieves for at least 48 h before use. Sieves were activated by heating under vacuum at 270 °C for at least 72 h. All other reagents were purchased from commercial vendors and used as received.

2.4.3 X-ray Structure Determinations. X-ray diffraction studies were carried out on a Bruker SMART APEX Duo and Kappa Duo diffractometer equipped with a CCD detector.[34] Measurements were carried out at -175 °C using Mo Kα (0.71073 Å) radiation and Cu Kα (1.54178 Å) radiation. Crystals were mounted on a glass capillary or Kaptan Loop with Paratone-N oil. Initial lattice parameters were obtained from a least squares analysis of more than 100 centered reflections; these parameters were later refined against all data. Data were integrated and corrected for Lorentz polarization effects using SAINT and were corrected for absorption effects using SADABS2.3. Space group assignments were based upon systematic absences, E statistics, and successful refinement of the structures. Structures were solved by direct methods with the aid of successive difference Fourier maps and were refined against all data using the SHELXTL 2014/7 software package. Thermal parameters for all non-hydrogen atoms were refined anisotropically. Hydrogen atoms, where added, were assigned to ideal positions and refined using a riding model with an isotropic thermal parameter 1.2 times that of the attached carbon atom (1.5 times for methyl hydrogens).

2.4.4 Preparation of Compounds. All manipulations were carried out under a dinitrogen atmosphere using standard Schlenk line and glovebox techniques. All chemicals were purchased from VWR International, Acros, Alpha Aesar, or Cambridge Isotopes. Bulk solvents were deoxygenated and dried by sparging with argon gas followed by passage through an activated alumina column. Deuterated solvents and other liquid reagents were degassed with dinitrogen and stored over activated 3 Å sieves prior to use. H_3ONO was synthesized in accordance with a reported procedure.[10]

$[(H_2ONO^-)_2Al][AlCl_4]$ (2.1). A solution of H_3ONO (259 mg, 1.22 mmol) in THF (2 mL) was held at -78°C while KH (58.1 mg, 1.45 mmol) was added. The solution was stirred for 1 hour as it warmed to room temperature and then cooled again to -78°C along with a solution of $AlCl_3$ (188 mg, 1.42 mmol) in THF (2 mL). The solution of "H_2ONO" was added to the stirring solution of $AlCl_3$ dropwise and warmed to room temperature with stirring over 2 hours. The resulting orange solution was evaporated to dryness, rinsed in 2 mL hexanes, extracted into 5 mL benzene, and filtered through Celite. The filtrate was evaporated to dryness to afford **2.1** as a light orange powder (263 mg, 70%). Crystals suitable for X-ray diffraction were grown from a concentrated toluene solution at -15°C overnight. ^1H NMR (400 MHz, C_6D_6) δ 5.18 (s, 2H, *CH*), 4.78 (d, J = 5.1 Hz, 2H, *NH*), 3.97 (dd, J = 19.1, 5.1 Hz, 2H, CH_2), 3.76 (d, J = 19.0 Hz, 2H,

CH_2), 1.16 (s, 20H, *$C(CH_3)_3$*), 0.74 (s, 19H, *$C(CH_3)_3$*). ^{13}C NMR (600 MHz, C_6D_6) δ 170.37, 100.25, 58.09, 43.39, 34.79, 27.92, 27.84, 25.28. IR (KBr; cm^{-1}): 3305 (w, NH), 3264 (m, NH), 3090 (w, CH), 2970 (s, CH), 2911 (m), 2873 (m), 1715 (m), 1657 (s, C=O), 1623 (m), 1480 (m), 1462 (m), 1414 (w), 1390 (m), 1370 (s), 1344 (m), 1297 (m), 1221 (m), 1161 (m), 1107 (m), 1095 (s, C-O). UV-vis spectrum (THF) λ_{max} (ε_M): 328 (2513), 447 (5770) nm (Lmol^{-1}cm^{-1}). Anal. Calcd. $C_{24}H_{44}Al_2Cl_4N_2O_4$: C, 46.49; H, 7.14; N, 4.52. Found: C, 43.55; H, 6.79; N, 4.04.

($HONO^{2-}$)AlCl(THF) (2.2). A solution of H_3ONO (295 mg, 1.39 mmol) in THF (2 mL) was held at -78°C while KH was added (128 mg, 3.19 mmol). The solution was stirred for 1 hour as it warmed to room temperature and then cooled again to -78 °C along with a solution of $AlCl_3$ (185 mg, 1.39 mmol) in THF (2 mL). The solution of "HONO" was added to the stirring solution of $AlCl_3$ dropwise and warmed to room temperature with stirring over 2 hours. The resulting purple solution was evaporated to dryness, extracted into hexane (5 mL) and filtered through Celite to remove salts. The filtrate was evaporated to dryness and 2.**2** was isolated as a light purple powder (357 mg, 75%). Crystals suitable for X-ray diffraction were grown by cooling a concentrated 1:1 hexane:toluene solution at -15°C overnight. ^{1}H NMR (400 MHz, C_6D_6) δ 4.87 (d, J = 1.99 Hz, 2H, *CH*), 4.04 (s, 4H, THF), 3.28 (s, 1H, *NH*), 1.17 (s, 22H, THF and *$C(CH_3)_3$*). ^{13}C NMR (600 MHz, C_6D_6) δ 168.14, 101.87, 71.51, 34.88, 27.97, 25.07. IR (KBr; cm^{-1}): 3271 (m, NH), 3098 (w, CH), 2963 (s), 2906 (m), 2869 (m), 1666 (w), 1642 (s), 1481 (m), 1458 (w), 1389 (m), 1356 (m), 1331 (s), 1219 (m), 1161 (m), 1131 (m), 1108 (m, C-O) 1092 (s), 1020 (s).UV-vis spectrum (THF) λ_{max} (ε_M): 308 (1251), 454 (105), 562 (28) nm (Lmol^{-1}cm^{-1}). Anal. Calcd. for $C_{16}H_{29}AlClNO_3$: C, 55.58; H, 8.45; N, 4.05. Found: C, 55.39; H, 8.08; N, 4.32.

[($HONO^{2-}$)Al]$_2$(μ-^{t}BuO)$_2$ (2.3). A solution of complex **2.2** (106 mg, 0.307 mmol) in THF (2 mL) was prepared. A second solution of ^{t}BuOK (37.4 mg, 0.333 mmol) in THF (1 mL) was then added to the first solution. The resulting blue solution was evaporated to dryness and extracted into benzene (5 mL) and filtered through Celite to remove salts. The filtrate was evaporated to dryness and **2.3** was isolated as a light blue powder (93.3 mg, 49%). ^{1}H NMR (400 MHz, C_6D_6) δ 4.96 (d, J = 2.17 Hz, 4H, *CH*), 3.60 (s, 2H, N-H), 1.49 (s, 18H, $C(CH_3)_3$), 1.21 (m, 36H, $C(CH_3)_3$). ^{13}C NMR (600 MHz, C_6D_6) δ 168.65, 99.93, 73.01, 34.62, 31.28, 27.79. IR (KBr: cm^{-1}): 3295 (w NH), 3093 (w, CH), 2963 (s), 2924 (m), 2905 (m), 2869 (m), 1642 (s), 1542 (w), 1481 (m), 1460 (m), 1421 (w), 1387 (m), 1370 (m), 1343 (s), 1240 (m), 1220 (s), 1183 (m), 1164 (m), 1142 (m), 1112 (m, C-O), 1030 (m), 1004 (s). UV-vis spectrum (THF) λ_{max} (ε_M): 323 (29), 457 (17) nm ($Lmol^{-1}cm^{-1}$). Anal. Calcd. $C_{32}H_{60}Al_2N_2O_6{\cdot}H_2O$: C, 59.98; H, 9.75; N, 4.37. Found: C, 59.65; H, 8.53 N, 4.47.

(HONO^{2-})Al(TEMPO)(TEMPOH) (2.4). A solution of complex **2.2** (44.5 mg, 0.129 mmol) in THF (1 mL) was prepared. A second solution of TEMPO (44.9 mg, 0.287 mmol) in THF (1 mL) was then added to the first solution. The resulting brown solution was evaporated to dryness and extracted into benzene (5 mL) and filtered through Celite. The filtrate was evaporated to dryness and **2.4** was isolated as a light brown powder (60.2 mg, 74 %). ^{1}H NMR (400 MHz, C_6D_6) δ 9.51 (s, 1H), 6.85 (s, 2H), 6.53 (s, 1H), 1.82 (s, 6H), 1.56 (d, J = 8.0 Hz, 6H), 1.38 (s, 14H), 1.17 – 1.12 (m, 30H). ^{13}C NMR (600 MHz, C_6D_6) δ 200.13, 116.28, 68.17, 60.05, 39.20, 38.25, 30.35, 27.14, 20.37, 19.95, 15.90. IR (KBr: cm^{-1}): 3403 (w, NH), 3255 (w, NH), 2961 (m, CH), 2927 (m), 2871 (m), 1567 (m), 1535 (m), 1460 (m), 1438 (m), 1421 (m), 1386 (m), 1375 (m), 1366 (m), 1298 (s), 1226 (m), 1103 (s, C-O), 1064 (m), 1014 (m). UV-vis spectrum (THF) λ_{max} (ε_M): 323 (1013), 434 (6829), 452 (6960) nm ($Lmol^{-1}cm^{-1}$). Anal. Calcd. $C_{30}H_{58}AlN_3O_4{\cdot}2H_2O$: C, 61.30; H, 10.63; N, 7.15. Found: C, 60.28; H, 10.04; N, 7.04.

2.5 Acknowledgements.

We thank Dr. James C. Fettinger for assisting in X-ray structure determination of complexes **2.1-2.4**. We thank the National Science Foundation for support of this work with award CHE-1763821. Preliminary results were obtained with support of a New Directions Grant from the University of California Davis Academic Senate. The National Science Foundation provided the Dual source X-ray diffractometer (CHE-1531193) and the NMR instrumentation (DBIO-722538).

This work can be found in the referenced publication: Phan, N.A., Fettinger, J.C. and Berben, L.A. A Ligand Protonation Series in Aluminum(III) Complexes of Tridentate Bis(enol)amine Ligand. *Organometallics.* **2018**, *37*, 4527-4533.

2.6 References.

[1] Culley, S. A.; Arduengo, A. J. Synthesis and Structure of the First 10-P-3 Species. *J. Am. Chem. Soc.* **1984**, *106*, 1164-1165.

[2] Culley, S. A.; Arduengo, A. J. The Synthesis and Structure of the First 10-As-3 species. *J. Am. Chem. Soc.* **1985**, *107*, 1089-1090.

[3] Arduengo, A. J.; Breker, J.; Davidson, F.; Kline, M. Dihalo Derivatives of 5-coordinate Hypervalent Phosphorus Compounds. *Heteroat. Chem.* **1993**, *4*, 213-221.

[4] Dunn, N. L.; Ha, M.; Radosevich, A. T. Main Group Redox Catalysis: Reversible P^{III}/P^{V} Redox Cycling at a Phosphorus Platform. *J. Am. Chem. Soc.* **2012**, *134*, 11330-11333.

[5] McCarthy, S. M.; Lin, Y.-C.; Devarajan, D.; Chang, J. W.; Yennawar, H. P.; Rioux, R. M.; Ess, D. H.; Radosevich, A. T. Intermolecular N-H Oxidative Addition of Ammonia, Alkylamines, and Arylamines to a Planar σ^3-Phosphorus Compound via an Entropy-Controlled Electrophilic Mechanism. *J. Am. Chem. Soc.* **2014**, *136*, 4640-4650.

[6] Lin, Y.-C.; Gilhula, J. C.; Radosevich, A. T. Nontrigonal Constraint Enhances 1,2-addition Reactivity of Phosphazenes. *Chem. Sci.* **2018**, *9*, 4338-4347.

[7] Stewart, C. A.; Harlow, R. L.; Arduengo, A. J. Chemistry and Structure of the First 10-Sb-3 Species. *J. Am. Chem. Soc.* **1985**, *107*, 5543-5545.

[8] Arduengo, A. J.; Stewart, C. A.; Davidson, F.; Dixon, D. A.; Becker, J. Y.; Culley, S. A.; Mizen, M. B. The Synthesis, Structure, and Chemistry of 10-Pn-3 Systems: Tricoordinate Hypervalent Pnictogen Compounds. *J. Am. Chem. Soc.* **1987**, *109*, 627-647.

[9] Driess, M.; Dona, N.; Merz, K. Novel Hypervalent Complexes of Main-group Metals by Intramolecular Ligand→Metal Electron Transfer. *Chem. - Eur. J.* **2004**, *10*, 5971-5976.

[10] Bettermann, G.; Arduengo, A. J. The Chemistry and Structure of a 10-Sn-4 System: Pseudo-trigonal-bipyramidal 4-coordinate, 10-electron Tin Centers. *J. Am. Chem. Soc.* **1988**, *110*, 877-879.

[11] Driess, M.; Muresan, N.; Merz, K. A Novel Type of Pentacoordinate Silicon Complexes and Unusual Ligand coupling by Intramolecular Electron Transfer. *Angew. Chem., Int. Ed.* **2005**, *44*, 6738-6741.

[12] Stewart, C. A.; Calabrese, J. C.; Arduengo, A. J. Synthesis and Structure of the First 20-Bi-9 System: A Discrete Nine-coordinate 20-electron Bismuth. *J. Am. Chem. Soc.* **1985**, *107*, 3397-3398.

[13] Arduengo, A. J., III; Stewart, C. A.; Davidson, F. Reversible transformation of 10-P-3 ADPO to an 8-P-3 ADPO·PtI_2 Adduct. *J. Am. Chem. Soc.* **1986**, *108*, 322-323.

[14] Arduengo, A. J.; Dias, H. V. R.; Calabrese, J. C. A Novel Mode of Coordination for Phosphorus. *J. Am. Chem. Soc.* **1991**, *113*, 7071-7072.

[15] Arduengo, A. J.; Lattman, M.; Calabrese, J. C.; Fagan, P. J. Complexes of Tricoordinate Hypervalent Pnictogens with (pentamethylcyclopentadienyl)ruthenium. *Heteroat. Chem.* **1990**, *1*, 407-417.

[16] Arduengo, A. J.; Lattman, M.; Dias, H. V. R.; Calabrese, J. C.; Kline, M. Pentacoordinate 10-electron Pnictogen-manganese Adducts: Verification of the 10-Pn-3 Arrangement in ADPnO Molecules. *J. Am. Chem. Soc.* **1991**, *113*, 1799-1805.

[17] Arduengo, A. J.; Dias, H. V. R.; Calabrese, J. C. Coordination Chemistry of ADPO. *Phosphorus, Sulfur Silicon Relat. Elem.* **1994**, *87*, 1-10.

[18] a) Thompson, E. J.; Berben, L. A. Electrocatalytic Hydrogen Production by an Aluminum(III) Complex: Ligand-Based Proton and Electron Transfer. *Angew. Chem., Int. Ed.* **2015**, *54*, 11642-11646. b) Sherbow, T. J.; Fettinger, J. C.; Berben, L. A. Control of Ligand pK_a Values Tunes the Electrocatalytic Dihydrogen Evolution Mechanism in a Redox-Active Aluminum(III) Complex. *Inorg. Chem.* **2017,** *56*, 8651-8660. c) Haddad, A. Z.; Garabato, B. D.; Kozlowski, P. M.;

Buchanan, R. M.; Grapperhaus, C. A. Beyond Metal-Hydrides: Non-Transition-Metal and Metal-Free Ligand-Centered Electrocatalytic Hydrogen Evolution and Hydrogen Oxidation. *J. Am. Chem*. Soc. **2016**, *138*, 7844-7847. d) Solis, B. H.; Maher, A. G.; Dogutan, D. K.; Nocera, D. G.; Hammes-Schiffer, S. Nickel Phlorin Intermediate Formed by Proton- Coupled Electron Transfer in Hydrogen Evolution Mechanism. *Proc. Natl. Acad. Sci. U. S. A.* **2016**, *113*, 485−492. e) Henthorn, J. T.; Lin, S.; Agapie, T. Combination of Redox-Active Ligand and Lewis Acid for Dioxygen Reduction with π-Bound Molybdenum−Quinonoid Complexes. *J. Am. Chem. Soc.* **2015**, *137*, 1458−1464.

[19] a) Myers, T. W.; Kazem, N.; Stoll, S.; Britt, R. D.; Shanmugam, M.; Berben, L. A. A Redox Series of Aluminum Complexes: Characterization of Four Oxidation States Including a Ligand Biradical State Stabilized via Exchange Coupling. *J. Am. Chem. Soc.* **2011**, *133*, 8662-8672. b) Myers, T. W.; Berben, L. A. Countercations Direct One- or Two-Electron Oxidation of an Al(III) Complex and Al(III)–Oxo Intermediates Activate C–H Bonds. *J. Am. Chem. Soc.* **2011**, *133*, 11865-11867.

[20] a) Myers, T. W.; Berben, L. A. Aluminum–Amido-Mediated Heterolytic Addition of Water Affords an Alumoxane. *Organometallics* **2013**, *32*, 6647-6649. b) Myers, T. W.; Berben, L. A. Aluminum–Ligand Cooperative N–H Bond Activation and an Example of Dehydrogenative Coupling. *J. Am. Chem. Soc.* **2013**, *135*, 9988-9990. c) Myers, T. W.; Berben, L. A. Aluminium-ligand Cooperation Promotes Selective Dehydrogenation of Formic Acid to H_2 and CO_2. *Chem. Sci.* **2014**, *5*, 2771-2777.

[21] a) Cole, B. E.; Wolbach, J. P.; Dougherty, W. G.; Piro, N. A.; Kassel, W. S.; Graves, C. R. Synthesis and Characterization of Aluminum-α-diimine Complexes over Multiple Redox States. *Inorg. Chem.* **2014**, *53*, 3899-3906. b) Wilson, H. H.; Koellner, C. A.; Hannan, Z. M.; Endy, C. B.; Bezpalko, M. W.; Piro, N. A.; Kassel, W. S.; Sonntag, M. D.; Graves, C. R. Synthesis and Characterization of Neutral Ligand α-Diimine Complexes of Aluminum with Tunable Redox Energetics. *Inorg. Chem.* **2018**, *57*, 9622-9633.

[22] a) Fedushkin, I. L.; Khvoinova, N. M.; Skatova, A. A.; Fukin, G. K. Oxidative Addition of Phenylacetylene through C-H Bond Cleavage To Form the Mg^{II}–dpp-Bian Complex: Molecular Structure of [Mg{dpp-Bian(H)}(C-CPh) $(thf)_2$] and Its Diphenylketone Insertion Product [Mg(dpp-Bian).–{OC(Ph_2)C-CPh}(thf)]. *Angew. Chem., Int. Ed.* **2003**, *42*, 5223-5226. b) Moskalev, M. V.; Lukoyanov, A. N.; Baranov, E. V.; Fedushkin, I. L. Unexpected Reactivity of an Alkylaluminum Complex of a Non-innocent 1,2-bis[(2,6-diisopropylphenyl)imino]acenaphthene Ligand (dpp-Bian). *Dalton Trans.* **2016**, *45*, 15872-15878.

[23] Szigethy, G.; Heyduk, A. F. Aluminum complexes of the redox-active [ONO] pincer ligand. *Dalton Trans.* **2012**, *41*, 8144-8152.

[24] Garrido, G.; Koort, E.; Rafols, C.; Bosch, E.; Rodima, T.; Leito, I.; Roses, M.J. *Org. Chem.* **2006**, *71*, 9062−9067.

[25] Chen, G.-Q.; Daniliuc, C. G.; Kehr, G.; Erker, G. Making Use of the Functional Group Combination of a Phosphane/Borane Lewis Pair Connected by an Unsaturated Four-Carbon Bridge. *Chem. - Eur. J.* **2017,** *2017*, 4519-4524.

[26] Isrow, D.; Captain, B. Synthesis and Reactivity of a Transition Metal Complex Containing Exclusively TEMPO Ligands: Ni(η2-TEMPO)2. *Inorg. Chem.* **2011,** *50*, 5864-5866.

[27] Liu, Y.-L.; Kehr, G.; Daniliuc, C. G.; Erker, G. Utilizing the TEMPO Radical in Zirconocene Cation and Hydrido Zirconocene Chemistry. *Organometallics* **2017,** *36*, 3407-3414.

[28] Hetterscheid, D. G. H.; Kaiser, J.; Reijerse, E.; Peters, T. P. J.; Thewissen, S.; Blok, A. N. J.; Smits, J. M. M.; de Gelder, R.; de Bruin, B. IrII(ethene): Metal or Carbon Radical? *J. Am. Chem. Soc.* **2005,** *127*, 1895-1905.

[29] Hodgson, J. L.; Namazian, M.; Bottle, S. E.; Coote, M. L. One-Electron Oxidation and Reduction Potentials of Nitroxide Antioxidants: A Theoretical Study. *J. Phys Chem. A.* **2007,** *111*, 13595-13605.

[30] Atkins, P. *Physical Chemistry*, 6th ed.; W. H. Freeman & Co.: New York, **1997**.

[31] Scepaniak, J. J.; Wright, A. M.; Lewis, R. A.; Wu, G.; Hayton, T. W. Tuning the Reactivity of TEMPO by Coordination to a Lewis Acid: Isolation and Reactivity of $MCl_3(\eta^1$-TEMPO) (M = Fe, Al) *J. Am. Chem. Soc.* **2012**, *134*, 19350.

[32] Addison, A. W.; Rao, T. N.; Reedijk, J.; Van Rijn, J.; Verschoor, G. C. Synthesis, structure, and spectroscopic properties of copper(II) compounds containing nitrogen–sulphur donor ligands; the crystal and molecular structure of aqua[1,7-bis(N-methylbenzimidazol-2′-yl)-2,6-dithiaheptane]copper(II) perchlorate. *J. Chem. Soc., Dalton Trans.* **1984**, 1349-1356.

[33] Connelly, N. G.; Geiger, W. E. Chemical Redox Agents for Organometallic Chemistry. *Chem. Rev*. **1996**, *96*, 877-910.

[34] (a) SMART Software Users Guide, Version 5.1, Bruker Analytical X-Ray Systems, Inc.; Madison, WI 1999. (b) SAINT Software Users Guide, Version 7.0, Bruker Analytical X-Ray Systems, Inc.; Madison, WI 1999. (c) G. M. Sheldrick, SADABS, Version 2.03, Bruker Analytical X-Ray Systems, Inc.; Madison, WI 2000. (d) G. M. Sheldrick, SHELXTL Version 6.12, Bruker Analytical X-Ray Systems, Inc.; Madison, WI 1999. (e) International Tables for X-Ray Crystallography, 1992, Vol. C., Dordrecht: Kluwer Academic Publishers.

Chapter 3: Synthesis of Unsupported Primary Phosphido Aluminum(III) Complexes

3.1 Introduction.

Materials containing element – phosphorous multiple bonds continue to receive interest for their promising materials properties.[1] Ongoing efforts to expand the scope of Group 13 – Group 15 containing species, with single, double, or triple bonds have resulted in many contributions to Al and Ga chemistry. Using the combination of Al and P has thus far led to the isolation of some terminal Al-phosphido complexes which contain an Al-P single bond. Of those terminal Al-phosphido containing molecules, most contain phosphido ligands that are well protected by two large R groups on the phosphide ligand, as in LAl-PR_2 and a majority of those secondary phosphido complexes are further protected by coordination of a Lewis base to the Al center.[2] Representative examples of Lewis base-free Al complexes having the form LAl-PR_2 include those with R = $SiPh_3$ reported by Power and coworkers,[3] R = $SiMe_3$ reported by Paine and coworkers,[4] and those with R = PPh_2 which was reported by Siefert and coworkers.[5] In each of those cases the ancillary L ligands comprise either one or two bulky *N*-donor ligands.

A less common moiety in Al-phosphido chemistry is the "LAl-PHR" core, where only one bulky R group protects the primary phosphide and L is a bidentate ligand. Lewis base-stabilized primary phosphido complexes have been reported.[6] along with just one report that is Lewis base-free. Tokitoh and coworkers have described two examples where R = 2,4,6-tri-*tert*-butylphenyl which is denoted as Mes*. The terminal phosphido P(H)Mes* is supported by a Lewis base-free Al center, Mes*(Cl)Al-, in Mes*(Cl)-Al-P(H)Mes* and in Mes*Al-$(P(H)Mes^*)_2$: both of these compounds contain three-coordinate Al centers.[7] In a later report, a further Lewis base stabilized complex was reported with the form Bbp(Br)(NHC)Al-P(H)Mes, where Bbp = 2,6-$[CH(SiMe_3)_2]_2C_6H_3$, NHC = *N*-heterocyclic carbene, and Mes = 2,4,6-trimethyphenyl.[8] An Al-phosphido double bond has been reported using bulky ligands to protect both the Al and P atoms,[9] and one reason that the Al-P(H)R functionality is targeted in other work is that it is seen as a precursor for a deprotonation or H-atom abstraction reaction to potentially afford an alternative route to the Al-P double bond.

Possible Al-P double bond routes

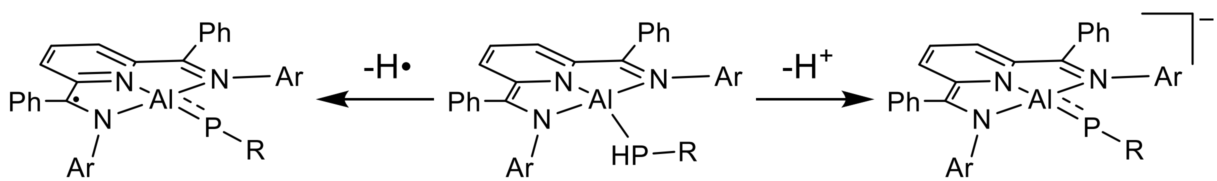

(I_2P^-)AlPR **(I_2P^{2-})AlP(H)R** **[(I_2P^{2-})AlPR]$^-$**

Scheme 3.1. Possible Al—P double bond routes from precursor (I_2P^{2-})AlP(H)R. Deprotonation of the phosphido ligand would generate an anionic complex. H-atom abstraction would generate a ligand radical complex, which monoanionic I_2P ligand complexes have demonstrated being able to support.

The square planar (SP) di(imino)pyridine (I_2P) Al complexes, denoted as (I_2P^{2-})AlX, where X = H, Cl, or I, were previously reported, and present an unusual geometry for a molecular main group species.[10,11] The chemical reactivity properties and theoretical work that has been communicated regarding these complexes suggests that the Al atom has an empty molecular orbital which is perpendicular to the square plane.[10-12] Analogous SP Ga complexes display similar electronic and reactivity properties.[11] In the present work we explore ligand substitution reactions at the Al center in SP complexes, and we also explored the nature of the empty orbital on Al and whether it can be exploited to access Al-ligand bonds with π-symmetry that contribute to Al-ligand multiple bond character (Chart 3.1).

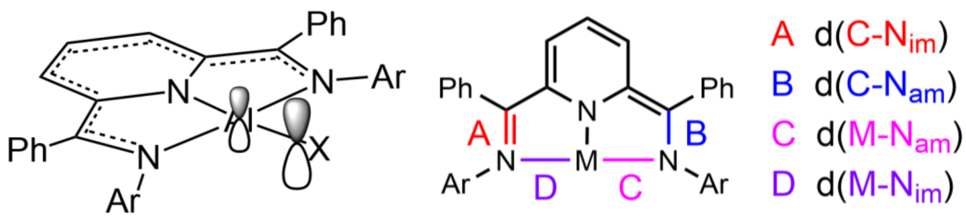

Chart 3.1. (left) Depiction of the possible *π*-symmetry donation from X-ligand into the SP I_2P^{2-} AlX complexes (X= P(H)Mes, P(H)Ph, Cl, or I). (right) Atom labelling scheme used in the manuscript discussion.

3.2 Results and Discussion.

3.2.1. Synthesis of Compounds. In both of the reports by Tokitoh and coworkers a salt metathesis reaction route was employed where reaction between an Al halide and a lithium phosphide results in formation of an Al-phosphido, following work-up to remove the lithium salt by-products.[7,8] Similar approaches to the synthesis of terminal phosphides have been employed in transition element chemistry such as in the reports of nickel-phosphido complexes, which were reported by Hillhouse and coworkers in 2002.[13] We followed a similar approach and set out to synthesize Al complexes of primary phosphido ligands via salt metathesis of (I_2P^{2-})AlX with LiPHMes or LiPHPh, where X = Cl or I. The lithium salts of a phosphide, LiPHMes and LiPHPh, were generated *in situ* from the addition of one equivalent ^{n}BuLi to either PH_2Mes or PH_2Ph, respectively, in an Et_2O solution at -68 ºC in a dry-ice acetone cold well. Our initial attempts explored dropwise addition of the LiPHMes or LiPHPh solutions to ($_{dipp}I_2P^{2-}$)AlCl but it quickly became apparent that no reaction was occurring under those conditions. We turned instead to reactions of LiPHMes or LiPHPh with the iodo complex, ($_{dipp}I_2P^{2-}$)AlI because iodo is often a better leaving group than chloro, and because the Al-I bond should be weaker. Dropwise addition of Et_2O solutions of LiPHMes or LiPHPh to ($_{dipp}I_2P^{2-}$)AlI, also dissolved in Et_2O, afforded an immediate color change. Following removal of the ethereal solvent in vacuo, and extraction of the products into benzene and into hexanes, sequentially, to remove the LiI, we obtained ($_{dipp}I_2P^{2-}$)Al(PHMes) (**3.1**) and ($_{dipp}I_2P^{2-}$)Al(PHPh) as dark brown-orange powders (Scheme 3.2). We were able to fully characterize **3.1** however, only the proton NMR spectrum of ($_{dipp}I_2P^{2-}$)Al(PHPh) was obtained (Figure 3.1), and further confirmation of the identity of ($_{dipp}I_2P^{2-}$)Al(PHPh) was elusive.

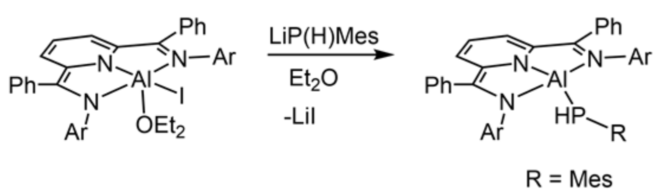

Scheme 3.1. Synthesis of **3.1**. Ar = 2,6-diisopropyphenyl (diip). R = mesityl (mes).

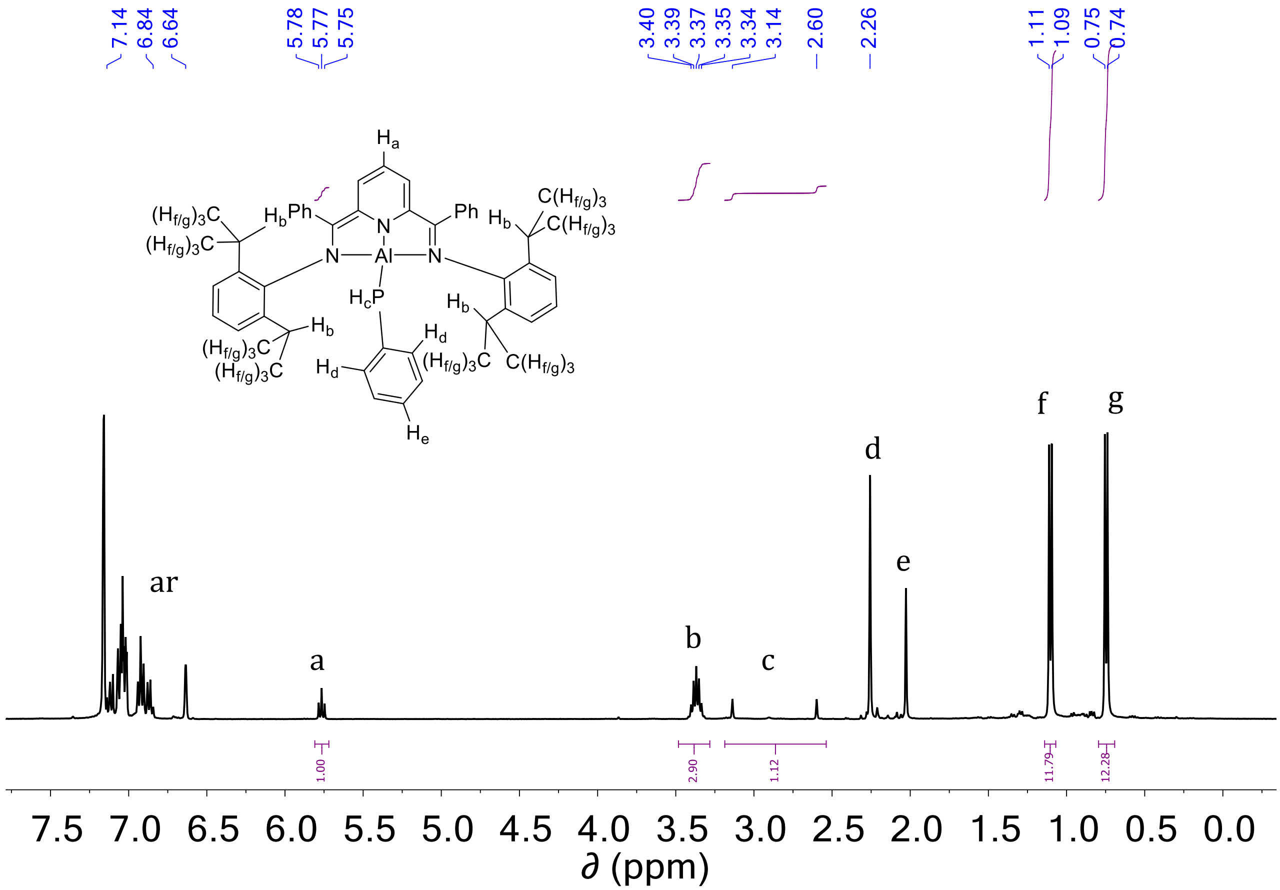

Figure 3.1. ^{1}H NMR spectrum of ($_{dipp}I_2P^{2-}$)Al(PHMes) (**3.1**)

Characterization of **3.1** was performed using ^{1}H-, ^{13}C-, and ^{31}P-NMR spectroscopy (Figure 3.1), along with single crystal X-ray crystallographic analysis of **3.1** which is described in more detail below. The proton NMR spectrum for compound **3.1** shows a triplet resonance at 5.77 ppm corresponding to its *para*-pyridine resonance and this represents a shift of 0.20 ppm upfield compared with the resonance at 5.97 ppm in ($_{dipp}I_2P^{2-}$)AlI. The (P)*H* resonance is observed as a doublet at 2.97 ppm with a large coupling constant of $^{1}J_{PH}$ = 215 Hz, and when the decoupled ^{31}P-NMR spectrum is acquired, a doublet is observed at -176 ppm with $^{1}J_{PH}$ = 215 Hz. This combined data suggests that the NMR signals for the two atoms are coupled to each other and that only one phosphorous containing compound, **3.1**, was synthesized. Compound **3.1** was not stable when stored outside the glove-box freezer and thus combustion analysis was not obtained. Additionally, attempts to obtain high-resolution mass spectra for **3.1** were also unsuccessful.

In **3.1** the I_2P ligand and the primary phosphido ligand both contain relatively bulky functional Ar and R groups, 2,6-diisopropyl phenyl and mesityl, respectively (Scheme 3.2) and so we reasoned that those groups might contribute to the instability of **3.1** and they might also contribute to lengthening of the Al-P bond in **3.1**. To test this hypothesis we synthesized an analog of the I_2P ligand where the 2,6-diisopropylphenyl substituents are replaced with the smaller 2,6-dimethylphenyl (xy) substituents, and we sought out the analogous complex ($_{Xyl}I_2P^{2-}$)AlI following a synthetic procedure identical to the one that was used to obtain ($_{Xyl}I_2P^{2-}$)AlI.[11] Unfortunately, we were not able to reliably isolate ($_{Xyl}I_2P^{2-}$)AlI in good yields and with a clean proton NMR spectrum. We did obtain confirmation of the identity of that compound from the crystallization of the compound from a concentrated toluene solution (Figure 3.2, Tables 3.1, 3.2). The single crystal X-ray diffraction study indicated that an ether molecule is bound to the Al center, and that the compound is ($_{Xyl}I_2P^{2-}$)AlI(Et_2O) (*vide infra*).

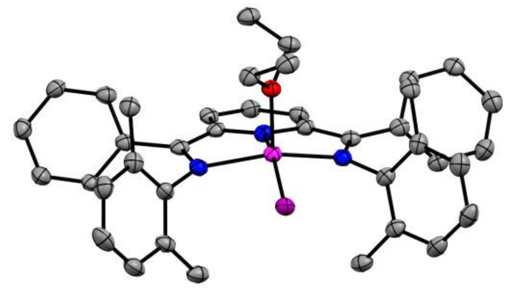

Figure 3.2. Solid-state structure of ($_{Me}I_2P^{2-}$)Al(Et_2O)I. Pink, blue, purple, red, and grey ellipsoids represent Al, N, I, O, and C atoms, respectively. Ellipsoids are shown at 30% probability level and H atoms have been omitted for clarity.

To circumvent our inability to isolate ($_{Xyl}I_2P^{2-}$)AlI(Et_2O), we performed a reaction where ($_{Xyl}I_2P^{2-}$)AlI(Et_2O) was generated in situ in Et_2O and then a suspension of LiP(H)Ph, also generated in Et_2O, was added dropwise to the solution of "($_{Xyl}I_2P^{2-}$)AlI(Et_2O)". The resulting primary phosphido complex was isolated in 80% yield and identified as ($_{Xyl}I_2P^{2-}$)Al(PHPh) (**3.2**) (Scheme 3.3).

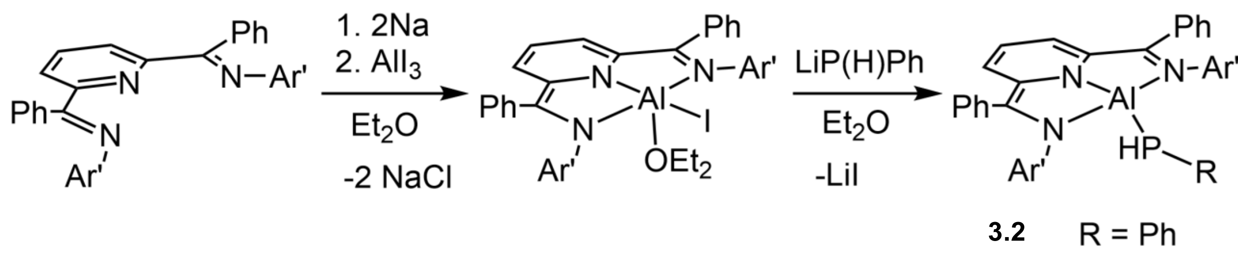

Scheme 3.3 Preparation of **3.2**. Ar′ = 2,6-dimethylphenyl (xy), R = phenyl (Ph).

Characterization of **3.2** was performed using ^{1}H-, ^{13}C-, and ^{31}P-NMR spectroscopy (Figure 3.3), along with single crystal X-ray crystallographic analysis of **3.2** which is described in more detail below. The proton NMR spectrum for compound **3.2** shows a triplet resonance at

6.29 ppm corresponding to its *para*-pyridine resonance and this represent a shift of 0.52 ppm downfield compared with the resonance at 5.77 ppm in **3.1**. The (P)*H* resonance is observed as a doublet at 3.20 ppm with a large coupling constant of $^{1}J_{PH}$ = 224 Hz, and when the decoupled ^{31}P-NMR spectrum is acquired, a doublet is observed at -141 ppm with $^{1}J_{PH}$ = J = 219 Hz. Despite the differences in steric bulk and electronic properties between **3.1** and **3.2**, compound **3.2** was also not particularly stable at room temperature for long periods and we were unable to obtain combustion analysis or a high-resolution mass spectrum.

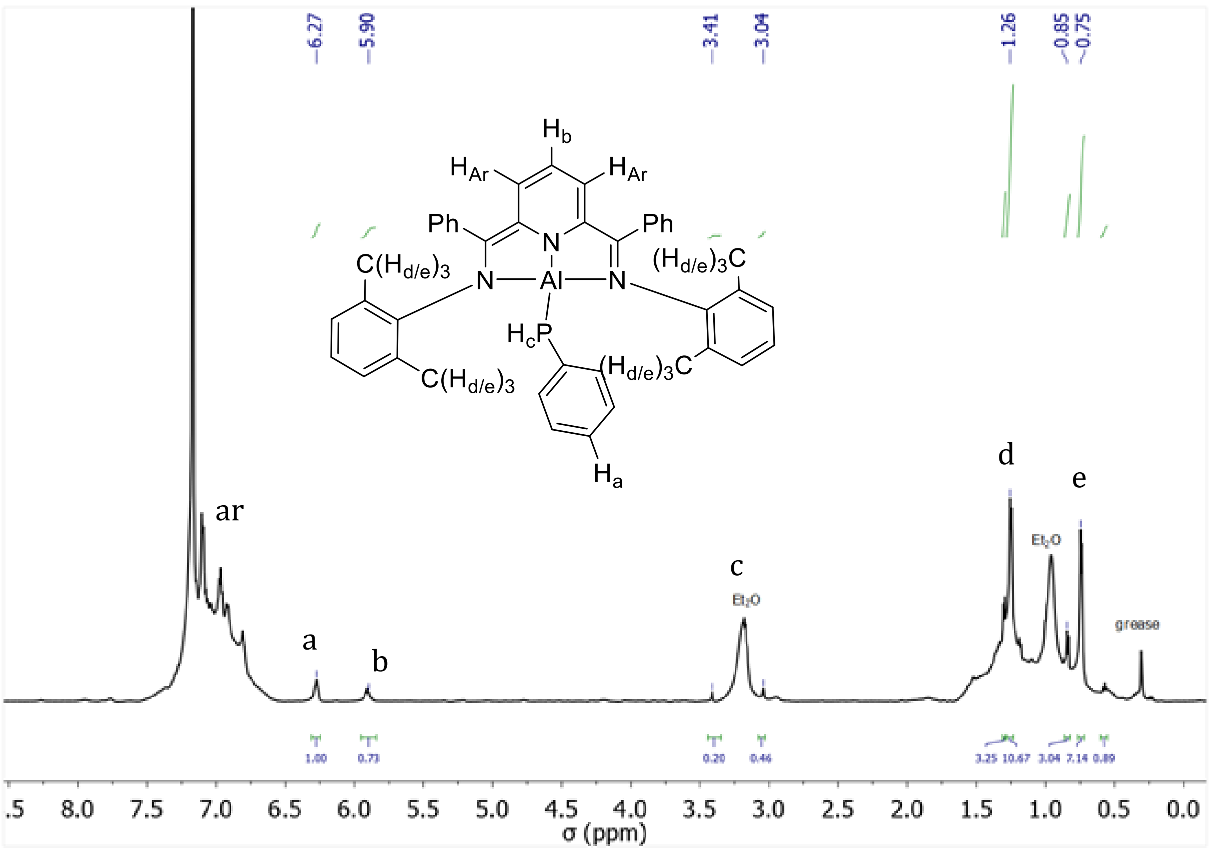

Figure 3.3. ^{1}H NMR spectrum of $(_{xy}I_2P^{2-})Al(PHPh)$ (**3.1**)

We also compared the ^{31}P-NMR chemical shifts for **3.1** and **3.2** to those that were previously reported for the Al complexes of primary phosphido complexes, by Tokitoh and coworkers. Those ^{31}P-NMR spectroscopic resonances were observed at -120 ppm ($^{1}J_{PH}$ = 222 Hz) and at -133 ppm ($^{1}J_{PH}$ = 210 Hz) for Mes*(Cl)-Al-(P(H)Mes*)$_2$ and Mes*(Cl)-Al-P(H)Mes*, respectively.[7]

Reactions with alkali metal bases were performed in attempts to remove H^+ from the -P(H)Mes and P(H)Ph moieties of **3.1** and **3.2**, respectively, with the goal that an Al-phosphinidene might be accessed. As an example of two separate reactions that were performed, one equivalent of benzyl potassium (C_7H_7K), or of *n*BuLi in toluene at -68 °C was stirred, with either **3.1** or **3.2**. In all cases a color change from a brown-orange to a red-brown solution was observed within 10 minutes. After removal of the solvent *in vacuo*, a solid product was obtained in each case and comprised about 40% of the original sample mass. The ^{31}P-NMR spectra of those solid products did not display any resonances and that suggested either no P-containing product had formed or that the product is paramagnetic. Unfortunately, all attempts to crystallize the reaction products were unsuccessful.

3.2.2. Solid State Structures. Single crystals of **3.1** and **3.2** were grown as brown cubes from concentrated hexanes or toluene solution, respectively, that was stored at -25 ºC overnight. (Figure 3.4, Tables 3.1 and 3.2). The neutral complexes have a four-coordinate Al center that is best described as distorted tetrahedral and consists of one tridentate I_2P^{2-} ligand and an anionic -PHR (R = Mes, Ph) ligand. The geometric structures of the ligands, $_{\rm diip}I_2P^{2-}$ and $_{\rm Xyl}I_2P^{2-}$, reveal an asymmetric structure with N_{im}—C_{im} and N_{am}—C_{am} bond lengths of 1.349(3) Å and 1.381(3) Å, respectively for **3.1** and bond lengths of 1.348(7) Å and 1.350(7) Å, respectively for **3.2** (see Chart 3.2 for atom labelling scheme) The asymmetry in the Al-N_{im} and Al-N_{am} bond lengths of **3.1**, which are 2.054(2) Å and 1.943(2) Å, respectively, and **3.2**, which are 1.943(4) Å and 1.836(5) Å, respectively, further confirms the asymmetry of the ligand electronic structure. The

C-C bond lengths around the edge of the ligand are best described as having alternating single and double bond character.

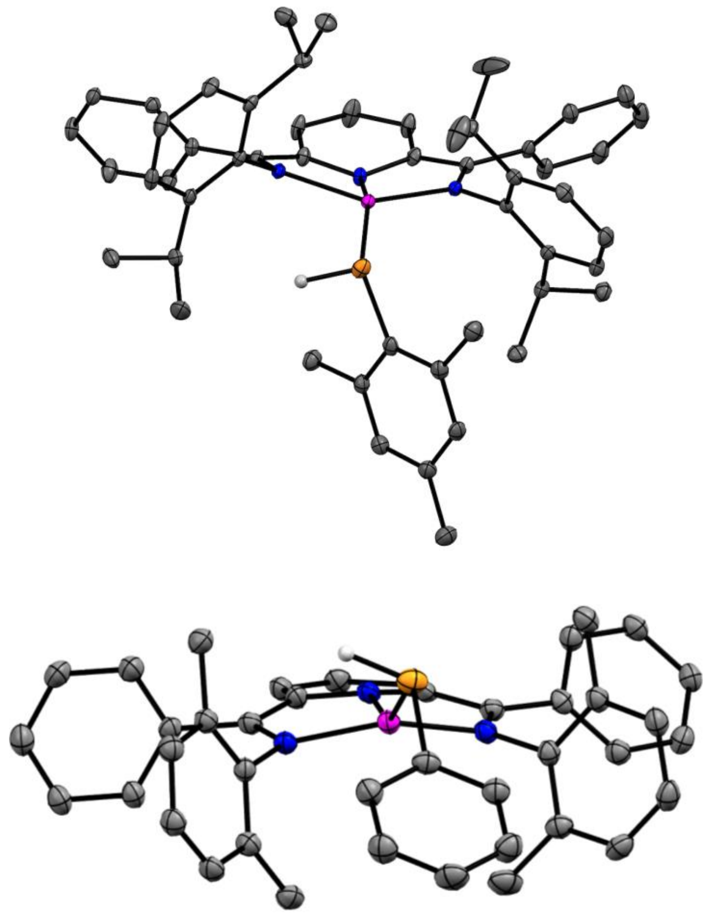

Figure 3.4. Solid-state structure of (top) $({}_{diip}I_2P^{2-})Al(PHMes)$ in **3.1**, and (bottom) $({}_{Xyl}I_2P^{2-})Al(PHPh)$ in **3.2**. Pink, blue, orange, and grey ellipsoids represent Al, N, P, and C atoms, respectively. Ellipsoids are shown at 30% probability level and H atoms, except (P)H have been omitted for clarity.

Table 3.1. Crystallographic data for ($_{xy}I_2P^{2-}$)AlI(Et_2O), **3.1**, and **3.2**.

	($_{xy}I_2P^{2-}$)AlI(Et_2O)	**3.1**	**3.2**
Formula	$C_{53}H_{57}AlIN_3O$	$C_{52}H_{59}AlN_3P$	$C_{41}H_{37}AlN_3P$
Crystal size	0.306 × 0.304 × 0.138	0.19 × 0.18 × 0.14	0.228 × 0.207 × 0.107
Formula wt., $gmol^{-1}$	905.89	783.97	629.68
Space group	*Pbca*	$P\bar{1}$	$P2_12_12_1$
a, Å	11.480(16)	10.9796(4)	7.3303(3)
b, Å	27.886(4)	13.3273(4)	18.6884(6)
c, Å	28.860(5)	16.0565(5)	23.9329(7)
α, deg	90	78.8627(16)	90
β, deg	90	78. 2135(17)	90
γ, deg	90	72.4072(16)	90
V, Å^3	9242(2)	2170.56(13)	3378.7(2)
Z	8	2	4
T, K	90(2)	100(2)	90(2)
ρ, calcd, g cm^{-3}	1.302	1.345	1.276
Refl. collected/$2\theta_{max}$	38139	16434	13148
Uniq refl./ $I > 2\sigma(I)$	8471/5448	8568/6618	5910/4302
No. param./restraints	540/0	549/30	423/1
λ, Å/μ (Kα), cm^{-1} [a]	1.54178	1.54178	1.54178
R_1/GOF[b]	0.0633/1.029	0.0566/1.057	0.0575/0.979
wR_2 ($I > 2\sigma(I)$)	0.1509	0.1261	0.1338
Resid density, eÅ^{-3}	1.798/-0.526	0.436/-0.400	0.582/-0.233

[a]Obtained with graphite-monochromated Cu Kα (λ = 1.54178 Å) radiation. [b]$R1 = \Sigma|| F_o | - F_c||/\Sigma|F_o|$, $wR2 = \{\Sigma[w(F_o^2 - F_c^2)^2]/\Sigma[w(F_o^2)^2]\}^{1/2}$.

Table 3.2. Selected bond distances and angles for ($_{xy}I_2P^{2-}$)AlI(Et_2O), **3.1**, and **3.2**.

	(xyI_2P^{2-})AlI(Et_2O)	**3.1**	**3.2**
Al—N_{im}	2.021(5)	2.054(2)	1.943(4)
Al—N_{am}	1.961(6)	1.943(2)	1.940(4)
Al—N_{py}	1.855(5)	1.831(2)	1.836(5)
Al—I	2.630(2)	N/A	N/A
Al—P	N/A	2.3423(12)	2.367(2)
N_{im}—C_{im}	1.365(7)	1.349(3)	1.348(7)
N_{am}—C_{am}	1.388(8)	1.381(3)	1.350(7)
N_{py}—$C_{py(o)}$	1.374(7)	1.376(3)	1.382(7)
N_{py}—$C_{py(o)'}$	1.385(8)	1.409(3)	1.403(6)
$C_{py(o)}$ —C_{im}	1.421(8)	1.431(3)	1.424(7)
C_{am}—$C_{py(o)'}$	1.422(8)	1.392(3)	1.415(7)
$C_{py(m)}$ —$C_{py(o)}$	1.365(9)	1.375(3)	1.370(9)
$C_{py(o)'}$—$C_{py(m)'}$	1.392(9)	1.394(3)	1.384(8)
$C_{py(p)}$ —$C_{py(m)}$	1.40(1)	1.395(4)	1.398(7)
$C_{py(p)}$ —$C_{py(m')}$	1.390(8)	1.371(4)	1.391(8)
N_{im}—Al—N_{py}	79.8(2)	80.55(8)	81.5(2)
N_{am}—Al—N_{py}	81.1(2)	83.18(8)	82.0(2)
N_{am}—Al—N_{im}	152.2(2)	151.28(8)	152.0(2)
N_{py}—Al—X [a]	165.0(2)	156.89(8)	144.3(2)
τ_4	N/A	0.367	0.452
τ_5	0.208	N/A	N/A

[a] For ($_{xy}I_2P^{2-}$)AlI(Et_2O), X = I; and for **1** and **2**, X = P.

The Al-P distances of 2.3423(12) in **3.1** and 2.367(2) Å in **3.2** fall within the ranges of Al-P bond lengths previously reported as single bonds. As examples, Mes*(Cl)-Al-P(H)Mes* which has a three-coordinate Al center has Al-P bond length 2.379(3) Å, and in Mes*Al-(P(H)Mes*)$_2$, which has a tetrahedral Al center, the two Al-P bond lengths are 2.405(2) and 2.417(2) Å.[7] Another four-coordinate Al center with terminal primary phosphide ligand, Bbp(Br)(NHC)Al-P(H)Mes, has Al-P bond length of 2.4074(6) Å,[7] although some other four-coordinate Al centers do show shorter Al-P bonds as in (dmap)Me$_2$Al–P(SiMe$_3$)$_2$ [P–Al 2.379(1) Å, dmap = 4-(dimethylamino)pyridine].[14] These comparisons indicate that the Al-P bond length in **3.1** (or **3.2**) is shorter than the Al-P bond lengths that have been observed for some other four-coordinate Al centers, and are instead more similar to the Al-P bond length found in three-coordinate Al complexes. Another example of an Al-P bond supported at a three-coordinate Al center is in Tip$_2$Al–P(SiPh$_3$)(1-adamantyl) [2.342(2) Å, Tip = 2,4,6-(iPr)$_3$C$_6$H$_2$], which is 1.342(2) Å.[3] Taken in the context of these previous reports, the Al-P bond lengths in **1** and **2** (at 2.3423(12) and 2.367(2) Å, respectively) are single bonds, and this is further consistent with the pyramidal geometry about each P atom in **3.1** and **3.2**.

The angles N_{py}-Al-P associated with each of **3.1** and **3.2** are 156.89(8) and 144.3(2) Å, respectively. In previous work describing square planar (SP) complexes of Al and Ga we have shown that the SP complexes, (I_2P^{2-})AlH and (I_2P^{2-})GaH, with σ-donor hydride ligands have N_{py}-Al-H or N_{py}-Ga-H angles of 180(1) and 177(11)°, respectively. In contrast, SP complexes containing a halide ligand have smaller angles that range from 167.01(4) to 168.78(19)° across the three compounds (I_2P^{2-})AlCl, (I_2P^{2-})AlI, and (I_2P^{2-})GaCl.[11,15] In the case of the halides and in the current case of the phosphide ligands there appears to be no steric driving force for the deviation from 180°. These smaller angles are therefore believed to derive from π-donation from the π-donor halide ligands, and from a π-donating contribution from the phosphido which is more effective when the π-symmetry orbital on the P atom approaches the empty orbital on Al more closely. The very weak π-donation, in the case of the Al-phosphido complexes may be the origin of the shortening of the Al-P bond lengths, by roughly 0.05 Å, relative to the Al-P bond lengths in other four-coordinate Al-phosphides (*vide supra*).[7]

The single crystal X-ray diffraction structure of ($_{Xyl}I_2P^{2-}$)AlI(Et_2O) revealed a similar electronic as the previously published ($_{dipp}I_2P^{2-}$)AlI.[11] The primary difference between the two compounds is that the former is five-coordinate with square pyramidal geometry and the latter is four-coordinate with square planar geometry. The ligand electronic structure in ($_{Xyl}I_2P^{2-}$)AlI(Et_2O) is best described as localized with alternating single and double bonds, and this is consistent with all of the other structures we have collected for square pyramidal complexes containing the $_{dipp}I_2P$ ligand.[16] For ($_{Xyl}I_2P^{2-}$)AlI(Et_2O), the two Al—N_{im} bonds differ in length and are 2.021(5) Å and 1.961(6) Å, whereas for SP ($_{dipp}I_2P^{2-}$)AlI the bond lengths are similar and are 1.945(5) Å and 1.965(5) Å. The Al—I bond in ($_{Xyl}I_2P^{2-}$)AlI(Et_2O) is 2.630(2) Å whereas in ($_{dipp}I_2P^{2-}$)AlI it is 2.556(19) Å. The longer Al—I bond in ($_{Xyl}I_2P^{2-}$)AlI(Et_2O) is consistent with the five-coordinate Al center as compared with the four-coordinate Al center in ($_{dipp}I_2P^{2-}$)AlI.

3.2.3. Electronic Spectra. Low energy, high extinction co-efficient absorption bands in planar metal-ligand complexes are often associated with a metalloaromatic electronic structure, and the observed transition is assigned to a metal-ligand charge transfer (MLCT) band. Characteristic MLCT absorption bands have been observed in square planar Al compounds of the di(imino)pyridine ligand where the absorption wavelength (and extinction coefficients) were 1041 (6900) and 1033 (4900) nm ($Lmol^{-1}cm^{-1}$), for (I_2P^{2-})AlCl and (I_2P^{2-})AlI, respectively.[11] In that prior work we also characterized the NIR region of the spectrum for one-electron oxidized compounds such as (I_2P^-))$AlCl_2$ and found no absorption band. Near infra-red (NIR) absorption spectra were collected for **3.1** and **3.2** and similar broad low energy bands were observed at 1042 (2489) and 1033 (1387) nm ($Lmol^{-1}cm^{-1}$), respectively (Figure 3.5). Each of these transitions is slightly lower in energy than those previously reported for (I_2P^{2-})AlCl and (I_2P^{2-})AlI, and the extinction coefficients are also lower suggesting that the transition is less allowed. Halide ligands such as chloro and iodo are π-donor in character. The phosphido ligands are likely weaker π-donors and this may result in the lowered electron density on the Al center and thus, the slightly lower energy for the observed MLCT absorption bands. Regardless of the exact details and comparisons, the observation of the low energy MLCT bands in **3.1** and **3.** is consistent with a persistent metalloaromatic structure for the (I_2P^{2-})AlX moiety across a range of X-type ligands including Cl^-, I^-, H^-, $^-$P(H)Ph, and $^-$P(H)Mes. The UV-Vis portion of the spectra for **3.1** and **3.2** show a broad band around 400 nm (~1800 – 3500 L $mol^{-1}cm^{-1}$) and we have previously assigned bands in this region to ligand-based π - π* transitions (Figure 3.6).

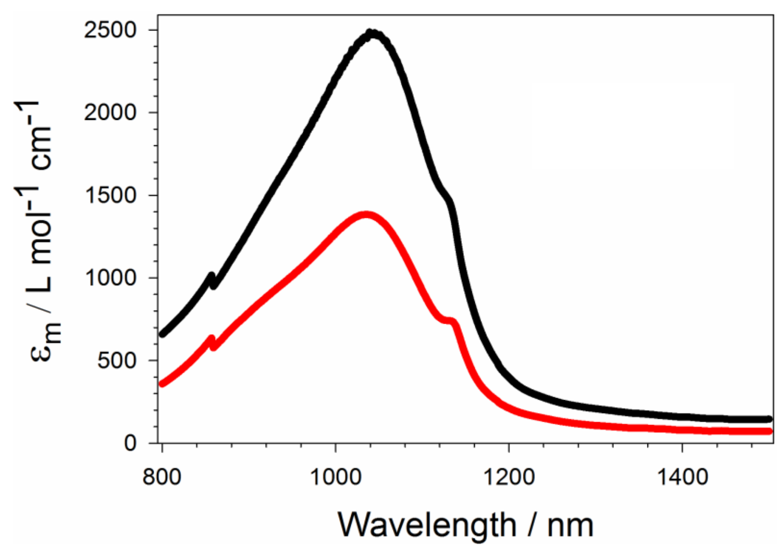

Figure 3.5. NIR spectra of 1.0 mM solutions of **3.1** (black), and **3.2** (red). All measurements recorded in C_6H_6. Discontinuities at 950 and 1120 nm are associated with lamp and detector changes in the instrument.

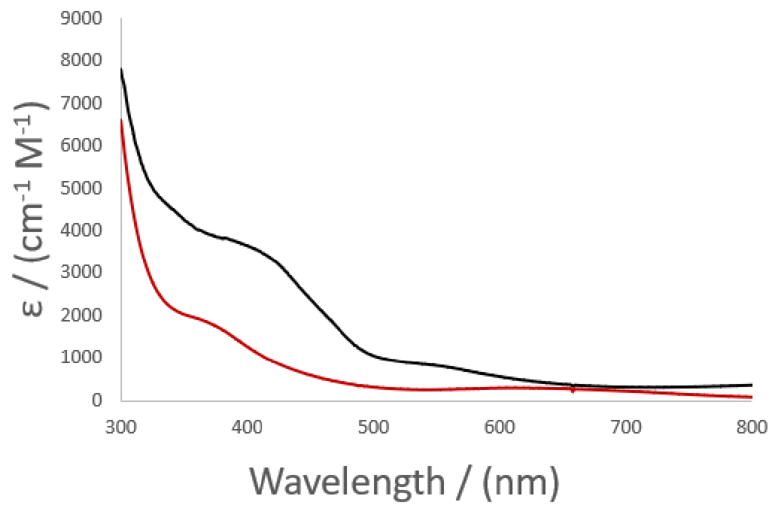

Figure 3.6. UV/ Vis spectrum of **3.1** (Black) and **3.2** (Red). All measurements recorded in C_6H_6.

3.3 Conclusion.

Two primary phosphido complexes of Al(III) have been isolated and characterized using single crystal X-ray diffraction, and ^{1}H-, ^{13}C-, and ^{31}P-NMR spectroscopy. The Al-P bond length in each of the complexes are consistent with single bond character. In addition, NIR spectroscopic measurements were used to characterize the metalloaromatic character in the Al-pincer ligand component of the molecule.

3.4 Experimental section.

3.4.1 Physical Measurements. ^{1}H-NMR, ^{13}C-NMR, ^{31}P-NMR, spectra were recorded at ambient temperature using a Varian 600 MHz or 400 MHz spectrometer. Chemical shifts were referenced to residual solvent. UV-Vis spectra were obtained using a 1 cm cuvette using an Agilent 8453 UV-vis spectrophotometer. Near infrared (NIR) spectra were collected using a Perkin Elmer Lambda 2050 UV-Vis-NIR spectrophotometer.

3.4.2 X-ray Structure Determinations. X-ray diffraction studies were carried out on a Bruker SMART APEX Duo or a Bruker Kappa Duo diffractometer equipped with a CCD detector.[17] Measurements were carried out at -175 °C using Cu Kα (1.54178 Å) radiation. Crystals were mounted on a glass capillary or Kaptan Loop with Paratone-N oil. Initial lattice parameters were obtained from a least-squares analysis of more than 100 centered reflections; these parameters were later refined against all data. Data were integrated and corrected for Lorentz polarization effects using SAINT,[18] and were corrected for absorption effects using SADABS2.3.[19] Space group assignments were based upon systematic absences, E statistics, and successful refinement of the structures. Structures were solved by direct methods with the aid of successive difference Fourier maps and were refined against all data using the SHELXTL 2014/7 software package.[20] Thermal parameters for all non-hydrogen atoms were refined anisotropically. Hydrogen atoms, where added and were assigned to ideal positions and refined using a riding model with an isotropic thermal parameter 1.2 times that of the attached carbon atom (1.5 times for methyl hydrogens).

3.4.3 Preparation of Compounds. All manipulations were carried out under a dinitrogen atmosphere using standard Schlenk line and glovebox techniques. All chemicals were purchased from VWR International, Acros, Alpha Aesar, or Cambridge Isotopes. Bulk solvents were deoxygenated and dried by sparging with argon gas followed by passage through an activated alumina column. Deuterated solvents and other liquid reagents were degassed with dinitrogen and stored over activated 3 Å sieves prior to use. Compounds $_{Xyl}I_2P$,[21] ($_{dipp}I_2P^{2-}$)AlI,[11] PH_2Mes,[22] and PH_2Ph,[23] were synthesized in accordance with reported procedures.

($_{dipp}I_2P^{2-}$)Al(PHMes) (3.1). Solid sodium (50.6 mg, 2.20 mmol) was stirred with $_{diip}I2P$ (493 mg, 1.00 mmol) in Et_2O (10 mL) for 24 hours after which the solution became a uniform intense blue color. One equivalent of AlI_3(0.408 mg, 1.0 mmol) was dissolved in 3 mL of Et_2O then added slowly to the blue solution of $Na_2({}_{diip}I_2P^{2-})$ at room temperature. The reaction solution turned red-brown and after stirring for thirty minutes. In a second reaction vessel, PH_2Mes (27.2 mg, 0.17 mmol) was dissolved in 5 mL Et_2O and cooled to -68 ºC in a dry-ice acetone cold well. Freshly titrated 2.9 M $^{n}BuLi$ (0.068 mL, 0.19 mmol) was added to the cold PH_2Mes solution resulting in the precipitation of a white solid and the evolution of butane. This slurry was added over 5 minutes to the first reaction vessel was left stirring for one hour during which time a color change from dark brown to a green-brown occurred. The Et_2O was removed *in vacuo* and then the solution was dissolved in benzene, filtered over Celite and the solvent was removed *in vacuo* leaving 1 as a brown powder (88 mg, 64%). Crystals suitable for X-ray diffraction were grown as brown cubes from a concentrated hexane solution stored at -25 ºC overnight. ^{1}H-NMR (600 MHz, C_6D_6): δ 7.14-6.84 (m, 18H, Ar, *m*-py), 6.64 (s, 3H, Mes), 5.77 (t, J = 7.7 Hz, 1H, *p*-py), 3.37 (hept, J = 6.7 Hz 4H, C*H*(CH_3)$_2$), 2.97 (d, J = 215.5 Hz, 1H, P*H*), 2.26 (s, 9H, Mes), 1.10 (d, J = 6.8 Hz, 6H, CH(CH_3)$_2$). 0.74 (d, J = 6.6 Hz 6H, CH(CH_3)$_2$). ^{31}P-NMR (243 MHz, C_6D_6): δ -176 (d, J = 215 Hz, *P*H). ^{13}C NMR (101 MHz, C_6D_6): δ 147.8, 143.9, 143.4, 141.7, 138.1, 135.0, 134.9, 134.6, 131.0, 130.4, 128.8, 128.6, 127.3, 126.5, 124.4, 119.1, 30.3, 26.2, 25.1, 24.2, 20.8. UV–vis-NIR spectrum (C_6D_6) λ_{max} (ε_M): 408 (3541), 1042 (2489) nm (L mol^{-1} cm^{-1}).

(${}_{Xyl}I_2P^{2-}$)AlI(Et_2O). Solid sodium (50.6 mg, 2.20 mmol) was stirred with ${}_{Xyl}I_2P$ (493 mg, 1.00 mmol) in Et_2O (10 mL) for 24 hours after which the solution became a uniform intense blue color. One equivalent of AlI_3 (0.408 mg, 1 mmol) was dissolved in 3 mL of Et_2O then added slowly to the blue solution of $Na_2({}_{Xyl}I_2P^{2-})$ at room temperature. The reaction solution turned red-brown and after stirring for thirty minutes, the solvent was removed in vacuo at room temperature. The residue was extracted into benzene (10 mL) and filtered through Celite to remove salts. The filtrate was evaporated to dryness. ($_{Xyl}I_2P^{2-}$)AlI(Et_2O) was obtained as a red-brown powder (476 mg, 66% yield). Crystals suitable for X-ray diffraction were grown from a concentrated toluene solution stored at -20 °C overnight. We were repeatedly unable to obtain a pure sample of ($_{Xyl}I_2P^{2-}$)AlI(Et_2O), and so we developed a synthesis of a phosphido complex where "($_{Xyl}I_2P^{2-}$)AlI(Et_2O)" was generated in situ and not isolated.

($_{Xyl}I_2P^{2-}$)Al(PHPh) (3.2). Solid sodium (25.8 mg, 1.12 mmol) was stirred with $_{Xyl}I_2P$ (230 mg, 0.47 mmol) in Et_2O (10 mL) for 24 hours after which the solution became a uniform intense blue color. One equivalent of AlI_3 (223 mg, 0.56 mmol) was dissolved in 3 mL of Et_2O then added slowly to the blue solution of Na_2($_{Xyl}I_2P^{2-}$) at room temperature. The reaction solution turned red-brown after stirring for thirty minutes. In a second reaction vessel, PH_2Ph (56.6 mg, 0.513 mmol) was dissolved in 5 mL Et_2O and cooled to -68 ºC in a dry-ice acetone cold well. Freshly titrated 2.9 M ^{n}BuLi (255 µL, 0.56 mmol in hexanes) was added to the cold PH_2Ph solution resulting in the precipitation of a white solid and the evolution of butane. This slurry was added dropwise over 5 minutes to the solution of "($_{Xyl}I_2P^{2-}$)Al-I(Et_2O)", and then the reaction mixture was left stirring for one hour while the color of the solution changes from dark brown to a green-brown. The Et_2O was removed *in vacuo* and then the solution was dissolved in benzene (10 mL), filtered over Celite and the solvent was removed *in vacuo* leaving 2 as a brown powder (234 mg, 80%). Crystals were grown as brown blocks from a concentrated toluene solution and stored at -25 ºC overnight .^{1}H-NMR (600 MHz, C_6D_6): δ 7.08-6.80 (m, 18H, Ar, *m*-py, PHC_6H_5), 6.27 (t, J =7.3 Hz, 1H, *p*-py, PHC_6H_5), 5.90 (t, *J* = 7.7 Hz, 1H, *p*-py), 3.20 (d, *J* = 224 Hz, 1H, P*H*), 1.26 (s, 6H CH_3). 0.75 (s, 6H, (CH_3). ^{31}P-NMR (243 MHz, C_6D_6): δ -141 (d, *J* = 219 Hz, *P*H). ^{13}C NMR (101 MHz, C_6D_6): δ 146.48, 145.98, 137.55, 135.82, 135.06, 134.92, 134.67, 134.28, 133.93, 133.50, 129.44, 128.89, 128.59, 127.67, 125.48, 118.47, 20.35. UV–vis-NIR spectrum (C_6D_6) λ_{max} (ε_M): 372 (1800), 1033 (1387) nm (L mol^{-1} cm^{-1}).

3.5 Acknowledgements.

Dr. Tobias J. Sherbow reported the initial synthesis and characterization of **3.1**.[24] We thank Prof. K. J. Koski for use of the UV-Vis-NIR spectrometer. We also thank Dr. James C. Fettinger for assisting in X-ray structure determination of complexes **3.1** and **3.2**. This manuscript is based on work supported by the National Science Foundation with award CHE-1763821.

This work can be found in the referenced publication: Phan, N.A., Sherbow, T.J., Fettinger, J.C. and Berben, L.A. Synthesis of Unsupported Primary Phosphido Complexes of Aluminum(III). *Z. Anorg. Allg. Chem.* **2021**. DOI: 10.1002/zaac.202100199.

3.6 References.

[1] K. L. Walz Mitra, C. H. Chang, M. P. Hanrahan, J. Yang, D. Tofan, W. M. Holden, N. Govind, G. T. Seidler, A. J. Rossini, A. Velian, *Angew. Chem. Int. Ed.* **2021**, *60*, 9127–9134.

[2] S. Aldridge, A. J. Downs, D. L. Kays in The Group 13 Metals Aluminium, Gallium, Indium and Thallium (Eds.: S. Aldridge, A. J. Downs), Wiley-VCH, Weinheim, **2011**, pp. 148–245.

[3] R. J. Wehmschulte, K. Ruhlandt-Senge, P. P. Power, *Inorg. Chem.* **1994**, *33*, 3205–3207.

[4] T. Habereder, H. Nöth, R. T. Paine, *Eur. J. Inorg. Chem.* **2007**, *28*, 4298–4305.

[5] K. Knabel, I. Krossing, H. Nöth, H. Schwenk-Kircher, M. Schmidt-Amelunxen, T. Seifert, *Eur. J. Inorg. Chem.* **1998**, *8*, 1095–1114.

[6] Lewis base coordinated phosphanylalumanes bearing P–H moieties: a) U. Vogel, A. Y. Timoshkin, M. Scheer, *Angew. Chem. Int. Ed.* **2001**, *40*, 4409-4412; *Angew. Chem*. **2001**, *113*, 4541-4544; b) V. Vogel, K.-C. Schwan, M. Scheer, *Eur. J. Inorg. Chem*. **2004**, *10*, 2062-2065; c) M. Bodensteiner, A. Y. Timoshkin, E. V. Peresypkina, U. Vogel, M. Scheer, *Chem. Eur. J.* **2013**, *19*, 957-963; d) M. Kapitein, C. von Hänisch, *Eur. J. Inorg. Chem*. **2015**, 5, 837-844; e) D. A. Atwood, L. Contreras, A. H. Cowley, R. A. Jones, M. A. Mardones, *Organometallics* **1993,** *12*, 17-18.

[7] J. T. Agou, S. Ikeda, T. Sasamori N. Tokitoh, *Eur. J. Inorg. Chem.* **2016,** *5*, 623-627.

[8] J. T. Agou, S. Ikeda, T. Sasamori, N.Tokitoh, *Eur. J. Inorg. Chem*. **2018**, *19*, 1984–1987.

[9] M. Fischer, S. Nees, T. Kupfer, J. T. Goettel, H. Braunschweig, C. Hering-Junghans, *J. Am. Chem. Soc.* **2021**, *143*, 4106–4111.

[10] E. J. Thompson, T. W. Myers, L. A Berben, *Angew. Chem. Intl. Ed.* **2014**, *53*, 14132-14134.

[11] T. M. Bass, C. R. Carr, T. J. Sherbow, J. C. Fettinger, L. A. Berben, *Inorg. Chem.* **2020**, *59*, 13517–13523.

[12] a) Z. Chen, W. Wang, C. Zhu, L. Wang, X. Fang, Y. Qiu, *Comput. Theor. Chem*. **2016**, *1090*, 129-133. b) W. Li, Y. Lyu, H. Zhang, M. Zhu, H. Tang. *Dalton Trans*. **2017**, *46*, 106-115.

[13] R. Melenkivitz, D. J. Mindiola, G. L. Hillhouse, *J. Am. Chem. Soc.* **2002**, *124*, 3846-3847.

[14] F. Thomas, S. Schulz, M. Niger, *Eur. J. Inorg. Chem*. **2001**, *1*. 161–166.

[15] E. J. Thompson, L. A. Berben, *Angew. Chem. Intl. Ed.* **2015**, *54*, 11642-11646.

[16] (a) T. W. Myers, L. A. Berben, *J. Am. Chem. Soc.* **2013**, *135*, 9988-9990. (b) T. W. Myers, T. J. Sherbow, J. C. Fettinger, L. A, Berben, *Dalton Trans.* **2016**, *45*, 5989-5998. (c) T. J. Sherbow, C. R. Carr, T. Y. Saisu, L. A. Berben, *Organometallics* **2016**, *35*, 9-14. (d) T. W. Myers, L. A. Berben, *Organometallics* **2013**, *32*, 6647-6649.

[17] *SMART Software Users Guide*, Version 5.1; Bruker Analytical X-Ray Systems, Inc.: Madison, WI **1999**.

[18] *SAINT Software Users Guide,* Version 7.0; Bruker Analytical X-Ray Systems, Inc.; Madison, WI **1999**.

[19] Sheldrick, G. M. *SADABS*, Version 2.03; Bruker Analytical X-Ray Systems, Inc.: Madison, WI, **2000**.

[20] Sheldrick, G. M. *SHELXTL*, Version 6.12; Bruker Analytical X-Ray Systems, Inc.: Madison, WI, **1999**.

[21] R. Schmidt, M. B. Welch, S. J. Palackal, H. G. Alt, *J. Mol. Catal. A: Chem*. **2002**, *179*, 155-173.

[22] Y. Takeda, T. Nishida, S. Minakata, *Chem. Eur. J.* **2014,** *20*, 10266-10270.

[23] C. E. Kefalidis, L. Perrin, C. J. Burns, D. J. Berg, L. Maron, R. A. Andersen, *Dalton Trans.* **2015,** *44*, 2575-2587.

[24] Sherbow, T.J. Synthesis and Electron, Proton Transfer Reactions of Bis(imino)pyridine and Bis(pyrazolyl)pyridine Aluminum(III) Complexes. Ph.D. Dissertation, University of California, Davis, Davis, CA, 2019.

Chapter 4: Electrochemical Characterization of $V\{N(SiMe_3)_2\}_3$

4.1 Introduction.

In 2019, the Power group at UC Davis published a new characterization of the transition metal complex $V\{N(SiMe_3)_2\}_3$.[1] $V\{N(SiMe_3)_2\}_3$ belongs to a class of metal trisilylamides with the formula $M\{N(SiMe_3)_2\}_3$ (M = 1st row transition metal), which are well known three-coordinate, open-shell transition metal complexes.[2-4] The first examples were reported in the early 1960s by Wannagat and Bürger[5,6] who synthesized $Cr\{N(SiMe_3)_2\}_3$[6] and $Fe\{N(SiMe_3)_2\}_3$.[7] Bradley and coworkers expanded the range of compounds to include metal trisylylamides with Sc, Ti, and V in the early 1970s.[8,9] In the late 1980s tris(silylamido) derivatives of manganese and cobalt were reported.[10] Since then X-ray crystal structures of the scandium,[11] titanium,[12] chromium,[13] manganese,[10] iron,[14,15] and cobalt[10] tris(silyamides) have been published as well. For the complex $V\{N(SiMe_3)_2\}_3$ (**4.1**) only some parameters of the structure (V–N, Si–N distances and Si–N–Si angle) were given in a review.[2] Full details of **4.1** have not been published until the publication from Power and coworkers in 2019.[1] In a previous publication, the preparation of $V\{N(SiMe_3)_2\}_3$ was described as a brown, crystalline solid.[16] The Power group synthesized $V\{N(SiMe_3)_2\}_3$ by following a route they previously described in a publication on low-coordinate amido derivatives of the early transition metals.[17] This resulted in their isolation of $V\{N(SiMe_3)_2\}_3$ as violet needles, different in color from the brown crystals that were previously described. The Power group provided full synthetic details of the violet color observed by Horvath and coworkers,[18] crystalline (**4.1**) product as well as its X-ray crystal structure and electronic and IR spectrum. In addition, the Power group described its reduction to the three-coordinate vanadium(II) species $[K(18\text{-crown-}6)(Et_2O)_2][V\{N(SiMe_3)_2\}_3]$(**4.2**) as well as the corresponding chromium(II) species [K(18-crown-6)(Et_2O)$_2$][Cr{N($SiMe_3$)$_2$}$_3$] (**4.3**). In order to assist with the characterization and elucidation of the electronic structure of **4.1-4.3**, I performed cyclic voltammetry (CV) measurements on the compounds.

4.2 Results and Discussion.

4.2.1. Electrochemical measurements. Electrochemical measurements were performed using cyclic voltammetry (CV) of complexes **4.1, [4.1$^-$],** Cr{N($SiMe_3$)$_2$}$_3$, and [Cr{N($SiMe_3$)$_2$}$_3$]$^-$ (Figure 4.1). The CV of **4.1** was performed in a 0.3 M Bu_4NPF_6/fluorobenzene solution and that of [**4.1**]$^-$, Cr{N($SiMe_3$)$_2$}$_3$, and [Cr{N($SiMe_3$)$_2$}$_3$]$^-$ in solutions of 0.3M Bu_4NPF_6/THF. When the reduction of **4.1** is performed in THF two reduction waves are observed indicating the possible formation of a THF complex with **4.1**. The open-circuit potentials of **4.1, [4.1$^-$],** Cr{N($SiMe_3$)$_2$}$_3$, and [Cr{N($SiMe_3$)$_2$}$_3$]$^-$ were measured as -0.95, -1.86, -0.65, and -1.43 V versus Fc/Fc^+, respectively. In the CV of **4.1** and [**4.1**]$^-$, a quasi-reversible couple is observed at -1.91 and -1.78 V, respectively, and is assigned to the $V^{III/II}$ couple. The $V^{III/II}$ couple potential in **4.1** and [**4.1**]$^-$ is significantly less reducing than the value for (nacnac)VCl(ODipp) (nacnac = [DippNC(CH_3)]$_2$CH; -2.14 V vs. Fc/Fc^+ in THF) which upon reduction also forms a three-coordinate vanadium(II) complex.[19] The CV Curves of Cr{N($SiMe_3$)$_2$}$_3$, and [Cr{N($SiMe_3$)$_2$}$_3$]$^-$ both have one quasi-reverisble redox couple at -1.48 V, corresponding to the $Cr^{III/II}$ couple. This is unlike the case of Cr{N($SiPr^i_3$)Dipp}$_2$ which shows an additional reduction wave at -2.04 V vs. Fc/Fc^+ demonstrating the feasibility of further reduction to Cr^I.[20]

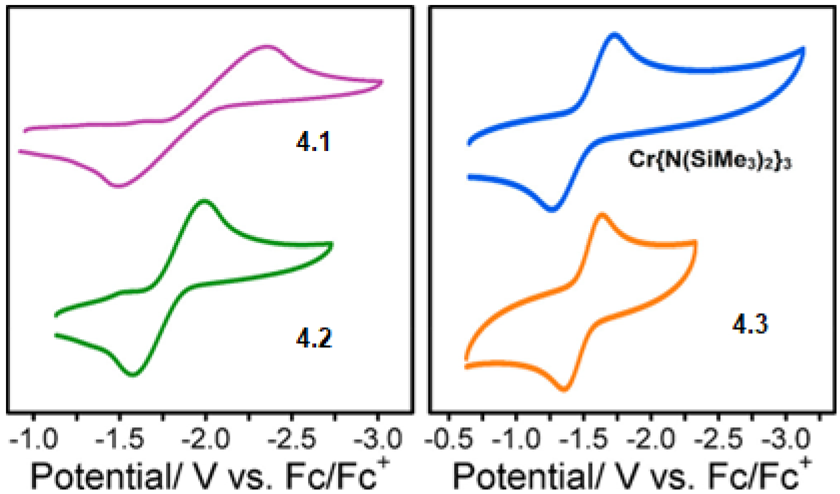

Figure 3.1. CV curves of 3.2 mM **4.1** (purple) in 0.3 M Bu_4NBF_4/fluorobenzene and 2.6 mM $[V\{N(SiMe_3)_2\}_3]^-$ (**4.2**; green), 2.6 mM $Cr\{N(SiMe_3)_2\}_3$ (blue), and 1.4 mM $[Cr\{N(SiMe_3)_2\}_3]^-$ (**4.3**; orange) in 0.3 M Bu_4NPF_6/THF. Scan rate = 200 mV s^{-1}, glassy carbon working electrode.

3.3 Conclusion.

The synthesis and characterization of **4.1** by the Power group repairs the long-held belief that **1** is a brown solid, and the definitive characterization may result in greater use of this compound as a synthon. The reduction of **4.1** results in a rare low-coordinate vanadium(II) species, [**4.1**]$^-$. The reduction of the chromium analogue results in the analogous charge-separated chromous salt.[21,22] Cyclic voltammograms of **4.1-4.3** assisted in the characterization of these products, describing their electrochemical properties.

4.4 Experimental section.

4.4.1 Electrochemical Measurements. Cyclic voltammograms were recorded in a nitrogen-filled glovebox in either 0.3 M Bu_4NBF_4 fluorobenzene solution or 0.3M Bu_4NPF_6 THF solution. A CH Instruments model 620D electrochemical analyzer with a glassy carbon working electrode (CH Instruments, nominal surface area of 0.071 cm2), a platinum wire auxiliary electrode, and a $Ag/AgNO_3$ (0.001M) nonaqueous reference electrode with a Vycor tip was used. Ferrocene was used as an internal standard and all potentials are referenced to the Fc/Fc^+ couple. Bu_4NBF_4 and Bu_4NPF_6 were recrystallized from ethanol and placed under vacuum for 72 h before electrolyte solutions were made. Electrolyte solutions were stored over 3 Å molecular sieves for at least 48 h before use. Sieves were activated by heating under vacuum at 270 °C for at least 72 h. All other reagents were purchased from commercial vendors and used as received.

4.5 Acknowledgements.

This work can be found in the referenced publication: Wagner, C. L.; Phan, N. A.; Fettinger, J. C.; Berben, L. A.; Power, P. P. New Characterization of $V\{N(SiMe_3)_2\}_3$: Reductions of Tris[bis(trimethylsilyl)amido]vanadium(III) and -chromium(III) To Afford the Reduced Metal(II) Anions $[M\{N(SiMe_3)_2\}_3]^-$ (M = V and Cr). *Inorg. Chem.* **2019**, *58*, 6095-6101.

4.6 References.

[1] Wagner, C. L.; Phan, N. A.; Fettinger, J. C.; Berben, L. A.; Power, P. P. New Characterization of $V\{N(SiMe_3)_2\}_3$: Reductions of Tris[bis(trimethylsilyl)amido]vanadium(III) and -chromium(III) To Afford the Reduced Metal(II) Anions $[M\{N(SiMe_3)_2\}_3]^-$ (M = V and Cr). *Inorg. Chem.* **2019**, *58*, 6095-6101.

[2] Eller, P. G.; Bradley, D. C.; Hursthouse, M. B.; Meek, D. Three Coordination in Metal Complexes. *Coord. Chem. Rev.* **1977**, *24*, 1-95.

---

[3] Cummins, C. C. Three-Coordinate Complexes of “Hard” Ligands: Advances in Synthesis Structure and Reactivity. *Prog. Inorg. Chem.* **1998**, *47*, 685-836.

[4] Alvarez, S. Bonding and stereochemistry of three-coordinated transition metal compounds. *Coord. Chem. Rev.* **1999**, *193-195*, 13-41.

[5] (a) Lappert, M. F.; Power, P. P.; Sanger, A. R.; Srivastava, R. C.; Metal and Metalloid Amides: Synthesis, Structures and Physical and Chemical Properties. *Horwood-Wiley*; Chichester. **1980** (b) Lappert, M. F.; Protchenko, A.; Power, P.P.; Seeber, A.; Metal Amide Chemistry. *John Wiley & Sons*; Chichester. **2008**.

[6] Bürger, H.; Wannagat, U. Silylamido Verbindungen von Chrom, Mangan, Nickel und Kupfer. *Monatsh. Chem.* **1964**, *95*, 1099-1102.

[7] Bürger, H.; Wannagat, U. Silylamido-Derivative von Eisen und Kobalt-Beitrage zur Chemie der Silicon-Stickstoff Verbindungen. *Monatsh Chem.* **1963**, *94*, 1007-1012.

[8] Bradley, D. C.; Copperthwaite, R. G. Three-co-ordinated Compounds of Titanium(III) and Vanadium(III). *Chem. Commun.* **1971**, 764.

[9] Alyea, E. C.; Bradley, D. C.; Copperthwaite, R. G. Three-co-ordinated Transition Metal Compounds. Part 1. The Preparation and Characterization of Tris(bistrimethylsilylamido)-derivatives of Scandium, Titanium, Vanadium, Chromium, and Iron. *J. Chem. Soc. Dalton* **1972**, 1580-1584.

[10] Ellison, J. J.; Power, P. P. First Examples of Three-Coordinate Manganese(III) and Cobalt(III): Synthesis and Characterization of the Complexes $M\{N(SiMe_3)_2\}_3$ (M = Mn or Co). *J. Am. Chem. Soc.* **1989**, *111*, 8044-8046.

[11] Ghotra, J. S.; Hursthouse, M. B.; Welch, A. J. Three-co-ordinate Scandium(III) and Europium(III): Crystal Structures of their Trishexamethyldisilylamides. *J. C. S. Chem. Commun.* **1973**, 669-670.

[12] Putzer, M. A.; Magull, J.; Goesmann, H.; Neumüller, B.; Dehnicke, K. Synthese, Eigenschaften and Kristallstructuren der Titan(III)–Amido–Komplexe $Ti[N(SiMe_3)_2]_3$, $[TiCl_2\{N(SiMe_3)_2\}(THF)_2]$ und $[Na(12\text{-Krone-4})_2][TiCl_2\{N(SiMe_3)_2\}_2]$. *Chem. Ber.* **1996**, *129*, 1401-1405.

[13] Köhn, R. D.; Kociok-Köhn, G.; Haufe, M. High Yield Synthesis of $[Cr\{N(SiMe_3)_2\}_3]$ and Accurate Structure Determination by Cocrystallization with Me_3Si_2. *Chem. Ber.* **1996**, *129*, 25-27.

[14] Bradley, D. C.; Hursthouse, M. B.; Rodesiler, P. F. The Structure of a Three Co-ordinate Iron(III) Compound. *Chem Commun*. **1969**, 14-15.

[15] Hursthouse, M. B.; Rodesiler, P. F. Crystal and Molecular Structure of Tris(hexamethyldisilylamido)iron(II). *J. C. S. Dalton*, **1972**, 2100-2102.

[16] Bradley, D. C.; Copperthwaite, R. G.; Extine, M. W.; Reichert, W. W.; Chisholm, M. H. Transition Metal Complexes of Bis(trimethylsilyl)amine (1,1,1,3,3,3-Hexamethyldisilazane). *Inorganic Syntheses* **1978**, *18*, 112-120.

[17] Boynton, J. N.; Guo, J. -D.; Fettinger, J. C.; Melton, C. E.; Nagase, S.; Power, P. P. Linear and Nonlinear Two-Coordinate Vanadium Complexes: Synthesis, Characterization, and Magnetic Properties of V(II) Amides. *J. Am. Chem. Soc.* **2013** *135*, 10720-10728.

[18] Horvath, B.; Strutz, J.; Geyer-Lippmann, J.; Horvath, E. G.; Preparation, Properties, and ESCA Characterization of Vanadium Surface Compounds on Silicagel. III. *Z. anorg. Allg. Chem.* **1981**, *483*, 205-218.

[19] Tran, B. L.; Pinter B.; Nichols, A. J.; Konopka F. T.; Thompson R.; Chen C.-H.; Krzystek, J.; Ozarowski, A.; Telser, J.; Baik, M.-H.; Meyer K.; Mindiola, D. J. A Planar Three-Coordinate Vanadium(II) Complex and the Study of Terminal Vanadium Nitrides from N_2: A Kinetic or Thermodynamic Impediment to N-N Bond Cleavage? *J. Am. Chem. Soc.* **2012**, *134*(31), 13035-13045.

[20] Cai, I. C.; Lipschutz, M. I.; Tilley, T. D. A Bis(amido) Ligand Set that Supports Two-coordinate Chromium in the +1, +2, and +3 Oxidation States. *Chem. Commun.* **2014** *50*, 13062-13065.

[21] Casey, A. T.; Clark, R. J. H.; Pidgeon, K. J. Various Transition Metal Compounds. *Inorg. Synth.* **1972**, *13*, 179– 181.

[22] Krüger, C. R.; Niederprüm, H.; Schmidt, M.; Scherer, O. Sodium Bis(trimethylsilyl)amide and Tris(trimethylsilyl)amine. *Inorg. Synth.* **2007**, *8*, 13– 19.

Appendix A: O-H Bond Activation by Di(imine)pyridine Complexes of Al(III) Substituted with Electron-Withdrawing Groups

A1 Introduction.

In the pursuit of catalytic chemical transformations like alcohol dehydrogenation and transfer hydrogenation, developing molecular compounds that can activate O—H bonds is the first step. Previously, di(imine)pyridine (I_2P) complexes of Al(III) have demonstrated O—H bond activation of phenols, benzyl alcohols, and primary alcohols via a metal-ligand cooperative pathway (Scheme A1).[1,2] ($_{Ph}I_2P$)AlH reacts with 1 equivalent of alcohols to afford a product with a protonated I_2P ligand and an alkoxide ligand. ($_{Ph}I_2P$)AlH reacts with 2 equivalents of alcohols to also afford a product with a protonated I_2P ligand and two alkoxide ligands with H_2 being liberated in the process.

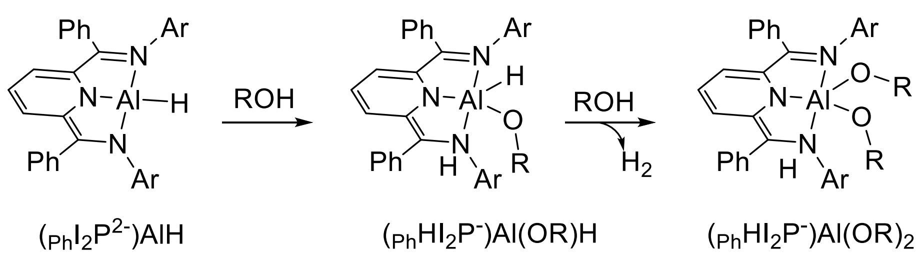

Scheme A1. Reaction of ($_{Ph}I_2P$)AlH with various alcohols (R = Ph, *p*-BnOMe, *p*-BnCF$_3$, *p*-BnOMe, ^{i}PrOH).

Building off established O—H bond activation work with I_2P Al complexes, a derivative of I_2P with electron-withdrawing pentafluorophenyl groups ($_{F5}I_2P$) was also explored (Scheme A2). After being reduced with two equivalents of sodium, $_{F5}I_2P$ reacts with $AlCl_3$ to form ($_{F5}I_2P$)AlCl(THF)$_2$.[3] An interesting feature of ($_{F5}I_2P$)AlCl(THF)$_2$ is the complex has two THF solvate ligands whereas ($_{Ph}I_2P$)AlCl(THF) only has one, a likely result of the electron-withdrawing I_2P ligand enabling a more Lewis acidic Al center that can support more ligands. When ($_{F5}I_2P$)AlCl(THF)$_2$ is compared to ($_{Ph}I_2P$)AlCl(THF), there is a dramatic shift in the $I_2P^{0/1-}$ redox potential. ($_{Ph}I_2P$)AlCl(THF) has a redox potential at -1.55 V vs. SCE [4] and ($_{F5}I_2P$)AlCl(THF)$_2$ has a redox potential at -1.16 V vs SCE, 390 mV more positive.

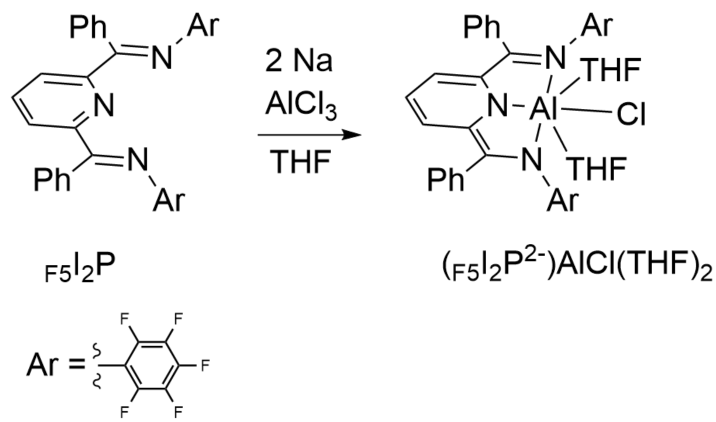

Scheme A2. Synthesis of ($_{F5}I_2P$)AlCl(THF)$_2$.

The incorporation of electron-withdrawing ligands has been a proven method to alter product formation, for example in Ni cross-coupling catalysis electron-withdrawing ligands can be designed to favor reductive elimination. [5] Exploring ($_{F5}I_2P$)AlCl(THF)$_2$'s reactivity in comparison to ($_{Ph}I_2P$)AlCl(THF) has potential to alter product formation due to the vast difference in electronic profile of supporting I_2P ligand, which is reflected in their respective redox potential. Additionally, the $_{F5}I_2P$ ligand has less steric bulk than $_{Ph}I_2P$ ligand which could play a role in the outer coordination sphere of the complexes. Reactions of ($_{F5}I_2P$)AlCl(THF)$_2$ with primary alcohols were explored to probe the complexes ability to activate O—H bonds. The $_{F5}I_2P$ ligand is more basic than the $_{Ph}I_2P$ ligand, given its' electron withdrawing groups, which may lead to contrasting reactivity with more acidic O—H bonds.

A2 Results and Discussion.

A2.1. Synthesis of Compounds. The synthesis of $_{F5}I_2P$ and $(_{F5}I_2P)AlCl(THF)_2$ were adopted from previously established procedure.[4,6] To explore the potential of $(_{F5}I_2P)AlCl(THF)_2$ to activate the O—H bonds of alcohols, reactions with methanol (MeOH) and isopropanol (^{i}PrOH) were conducted. The reactions were carried out in THF where MeOH or ^{i}PrOH were added dropwise to solutions of $(_{F5}I_2P)AlCl(THF)_2$ (Scheme A3). An immediate color change was observed with the addition of MeOH and ^{i}PrOH, where the solutions turned from red-brown to blue and blue-green, respectively. The reaction with MeOH formed product **A1** and the reaction with ^{i}PrOH formed product **A2**.

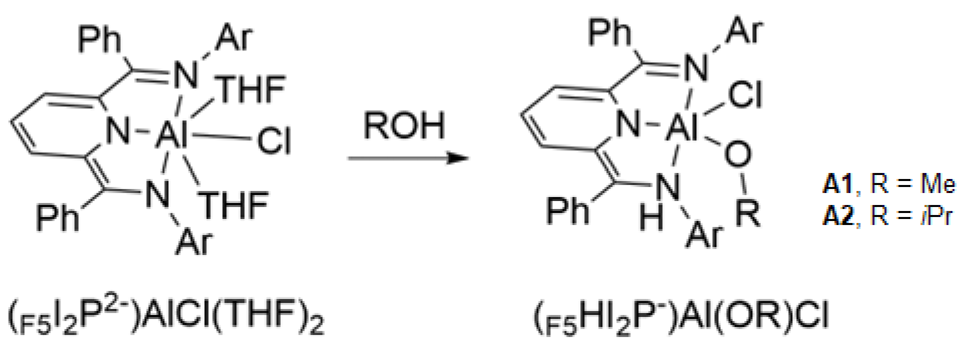

Scheme A3 Reaction of $(_{F5}I_2P)AlCl(THF)_2$ with alcohols (R = Me, *i*Pr) to form **A1** and **A2**.

A2.2. ^{1}H NMR Spectra. The ^{1}H NMR spectra reveals reactions of $(_{F5}I_2P)AlCl(THF)_2$ with MeOH and ^{i}PrOH occurred in an analogous manner of $(_{Ph}I_2P)AlH$ reacting with phenols and benzyl alcohols. The ^{1}H NMR spectrum of **A1** (Figure A1, middle) shows a singlet peak at 6.01 ppm, corresponding to the protonated amine, and a quartet at 5.68 ppm, corresponding to the *para*-pyridyl proton. These shifts are consistent with the previously reported protonated $_{Ph}I_2P$ complexes.[1,2] For **A2**, the analogous singlet appears at 5.99 ppm and the analogous quartet at

5.67 ppm. The emergence of a quartet for the *para*-pyridyl proton is expected as it indicates that the protonated H-I_2P ligand has an asymmetric electronic structure. This differs from the starting compound ($_{F5}I_2P$)AlCl(THF)$_2$'s *para*-pyridyl proton that appears as a triplet in the ^{1}H NMR spectrum at 5.30 ppm (Figure A1, top).

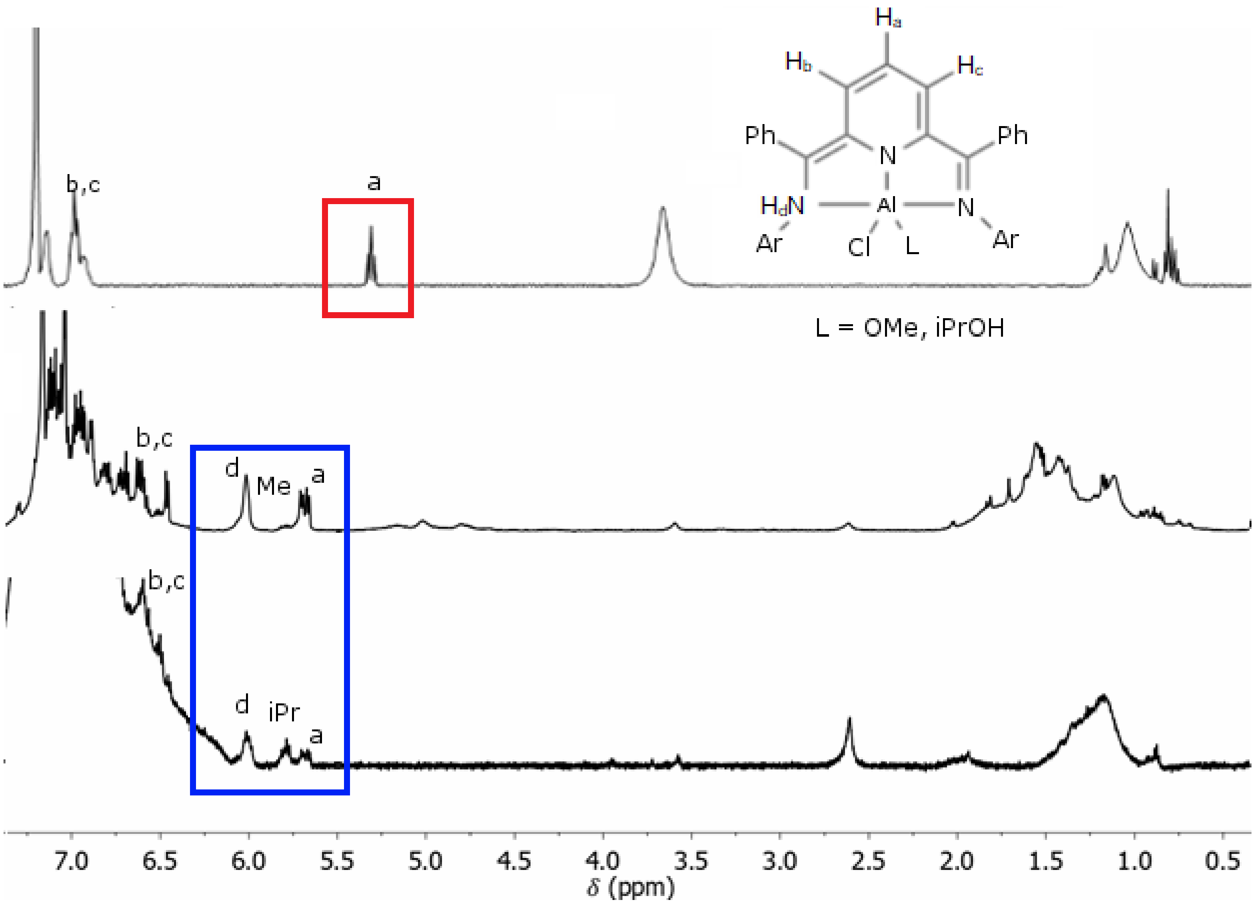

Figure A1 ^{1}H NMR spectrum of ($_{F5}I_2P$)AlCl(THF)$_2$ (top), **A1** (middle), and **A2** (bottom)**.** The labeled chemical structure corresponds to each spectrum. The red box (top) and blue box (middle, bottom) highlight the chemical shifts of the *para*-pyridyl proton of the ligand and how it changes from the I_2P^{2-} ligand charge state to HI_2P^-.

A3 Conclusion.

Two complexes with the protonated ${}_{F5}I_2P$ ligand have been identified by ^1H NMR via the reaction of $({}_{F5}I_2P)AlCl(THF)_2$ with MeOH and ^{i}PrOH. The observed O—H bond activation is consistent with previously reported Al ${}_{Ph}I_2P$ complexes.

A4 Experimental section.

A4.1 Physical Measurements. ^{1}H-NMR spectra were recorded at ambient temperature using a Varian 600 MHz spectrometer. Chemical shifts were referenced to residual solvent.

A4.2 Preparation of Compounds. All manipulations were carried out under a dinitrogen atmosphere using standard Schlenk line and glovebox techniques. All chemicals were purchased from VWR International, Acros, Alpha Aesar, or Cambridge Isotopes. Bulk solvents were deoxygenated and dried by sparging with argon gas followed by passage through an activated alumina column. Deuterated solvents and other liquid reagents were dried with calcium hydride, degassed with dinitrogen, and stored over activated 3 Å sieves prior to use.

$({}_{F5}HI_2P)AlCl(OMe)$ (A1). To a solution of $({}_{F5}I_2P)AlCl(THF)_2$ (202 mg, 0.245 mmol) dissolved in 5 mL of THF was added 1 equivalent of MeOH (9.94 μL) dropwise. The initial red-brown solution stirred for two hours, gradually turning blue. The reaction solvent was removed *in vacuo* and the resulting blue solid was dissolved in benzene and filtered over Celite. Compound **A1** was dried *in vacuo* and collected as a light blue powder (68 mg, 38.9% yield). ^{1}H

NMR spectrum was recorded in C_6D_6. ^{1}H-NMR (600 MHz, C_6D_6): δ 6.93-6.46 (m, 12H, Ar, *m*-py), 6.01 (s, 1H, NH), 5.80 (s, 3H, OMe), 5.68 (dd, *J* = 8.75 Hz, 1H, *p*-py).

($_{F5}$HI$_2$P)AlCl(O*i*Pr) (A2). To a solution of ($_{F5}$I$_2$P)AlCl(THF)$_2$ (204 mg, 0.248 mmol) dissolved in 5 mL of THF was added 1 equivalent of ^{i}PrOH (18.9 μL) dropwise. The initial red-brown solution stirred for two hours, gradually turning green-blue. The reaction solvent was removed *in vacuo* and the resulting green-blue solid was dissolved in benzene and filtered over Celite. Compound **A1** was dried *in vacuo* and collected as a light green-blue powder (144 mg, 78.5% yield). ^{1}H NMR spectrum was recorded in C_6D_6. ^{1}H-NMR (600 MHz, C_6D_6): δ 6.81-6.44 (m, 12H, Ar, *m*-py), 5.99 (s, 1H, NH), 5.78 (m, 3H, O^{i}Pr), 5.66 (dd, *J* = 8.19 Hz, 1H, *p*-py), 1.95 (br, 9H, O^{i}Pr) .

A5 Acknowledgements.

Dr. Tobias J. Sherbow reported the initial discovery of the synthesis and characterization of ($_{F5}$I$_2$P)AlCl(THF)$_2$. See reference 3.

A6 References.

[1] Sherbow, T. J.; Carr, C. R.; Saisu, T.; Fettinger, J. C.; Berben, L. A. Insight into Varied Reaction Pathways for O–H and N–H Bond Activation by Bis(imino)pyridine Complexes of Al(III). *Organometallics* **2016**, *35*, 9-14.

[2] Carr, C. R.; Vesto, J. I.; Xing, X.; Fettinger, J. C.; Berben, L. A. Aluminum-Ligand Cooperative O−H Bond Activation Initiates Catalytic Transfer Hydrogenation. *ChemCatChem* **2022**, *14*, e202101869.

[3] Sherbow, T.J. Synthesis and Electron, Proton Transfer Reactions of Bis(imino)pyridine and Bis(pyrazolyl)pyridine Aluminum(III) Complexes. Ph.D. Dissertation, University of California, Davis, Davis, CA, 2019.

[4] Thompson, E. J.; Berben, L. A. Electrocatalytic Hydrogen Production by an Aluminum(III) Complex: Ligand-Based Proton and Electron Transfer. *Angew. Chem., Int. Ed.* **2015**, *54*, 11642-11646.

[5] Mills, L. R.; Edjoc, R. K.; Rousseaux, S. A. L. Design of an Electron-Withdrawing Benzonitrile Ligand for Ni-Catalyzed Cross-Coupling Involving Tertiary Nucleophiles. *J. Am. Chem. Soc.* **2021**, *143*, 10422-10428.

[6] Kleigrewe, N.; Steffen, W.; Blömker, T.; Kehr, G.; Fröhlich, R.; Wibbeling, B.; Erker, G.; Wasilke, J.-C.; Wu, G.; Bazan, G. C. Chelate Bis(imino)pyridine Cobalt Complexes: Synthesis, Reduction, and Evidence for the Generation of Ethene Polymerization Catalysts by Li^+ Cation Activation. *J. Am. Chem. Soc.* **2005,** 127, 13955-13968.